1 **Structure and mechanism of bacterial tripartite efflux pumps**

2

3 Arthur Neuberger, Dijun Du and Ben F. Luisi[*]

4
5 Department of Biochemistry, University of Cambridge, Tennis Court Road, Cambridge CB2
6 1GA, UK
7
8 [*]To whom correspondence should be addressed. Email: bfl20@cam.ac.uk

9 **Abstract**

10 **Efflux pumps are membrane proteins which contribute to multi-drug resistance. In**
11 **Gram-negative bacteria, some of these pumps form complex tripartite assemblies in**
12 **association with an outer membrane channel and a periplasmic fusion protein. These**
13 **tripartite machineries span both membranes and the periplasmic space, and they**
14 **extrude from the bacterium chemically diverse toxic substrates. In this chapter, we**
15 **summarise current understanding of the structural architecture, functionality, and**
16 **regulation of tripartite multi-drug efflux assemblies.**

17

18 **Keywords: multi-drug efflux pumps, membrane proteins, antibiotic resistance,**
19 **tripartite assemblies**

20

21 **Introduction**

22 The tripartite efflux pumps of Gram-negative bacteria are complex molecular

23 assemblies that expel antibiotics and other toxic agents from the cell. The capacity of tripartite

24 systems to transport a variety of chemically diverse antibiotics and other bactericidal substrates

25 contributes to multi-drug resistance of Gram-negative bacteria and thus to the worldwide

26 emerging threat of untreatable infections (overview in [1]).

27 One well-studied representative of tripartite efflux pumps is the AcrA-AcrB-TolC

28 (hereafter AcrAB-TolC) assembly of *Escherichia coli*. The pump has become a paradigm

29 system to understand the structure and activities of homologous tripartite assemblies found in

30 phylogenetically diverse bacterial species, including those associated with clinical severity in

31 drug resistant infections [2-4]. Like numerous other tripartite systems, the AcrAB-TolC pump

32 spans the two lipid bilayers and an interstitial peptidoglycan network that together comprise

33 the cell envelope of the Gram-negative species. A nanomachine driven by proton-motive force,

34 AcrAB-TolC has been shown to transport antibiotics and a range of chemically diverse

35 bactericidal compounds [5, 6] [7] [8, 9]. Other tripartite systems drive efflux of more specific

36 compounds; for example, the CusA-CusB-CusC pump is involved in the efflux of toxic copper

37 and silver ions [10, 11].

38   The energy-transducing component of AcrAB-TolC system is the trimeric inner

39 membrane protein AcrB, which is a member of the Resistance-Nodulation-Cell division (RND)

40 superfamily. Tripartite assemblies can also form based on inner membrane transporters from

41 the major facilitator superfamily (MFS) and ATP-binding cassette (ABC) groups. A schematic

42 overview of different tripartite systems is displayed in Figure 1A-D.

43
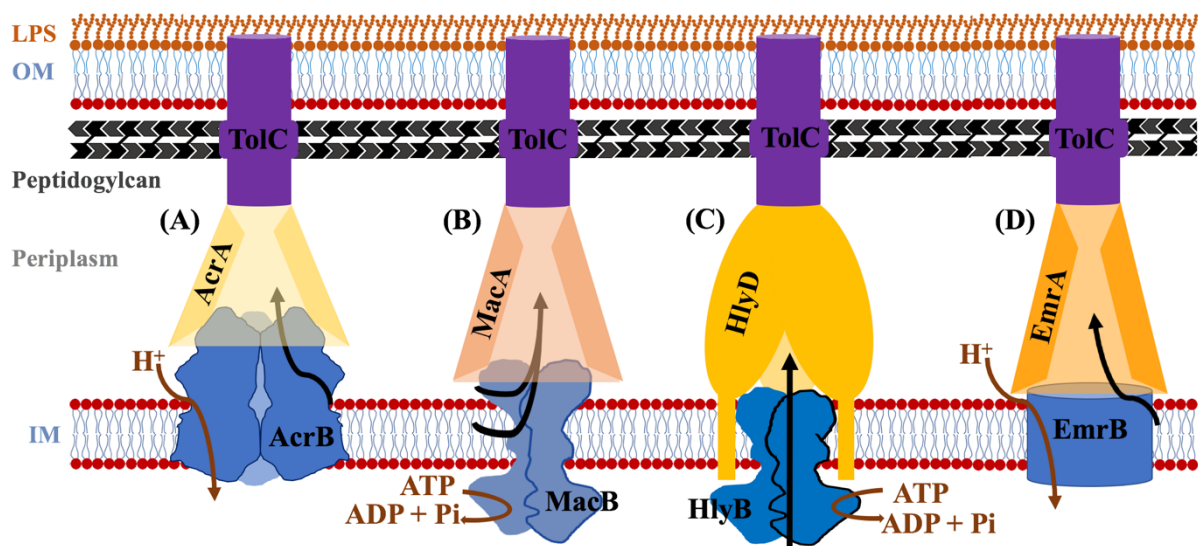
44

45 **Fig. 1. Schematic overview of the architecture of different tripartite systems.** (A) The

46 AcrAB-TolC tripartite assembly expels toxic substances utilizing the proton-motive force as

47 energy source by AcrB. Substrates are exported in exchange for the uptake of protons. (B)

48 MacAB-TolC drive transport by hydrolysis of ATP. (C) The type I secretion system HlyDB-

49   TolC shares some features with the MacAB-TolC system, although the intracellular ATPase

50   domain is elaborated with additional domains. (D) The EmrAB-TolC tripartite system. EmrB

51   is a member of the major facilitator superfamily of membrane transporters and utilises proton-

52   motive force for extrusion of toxic substrates. The structure of EmrB and subunit stoichiometry

53   of the EmrAB-TolC tripartite system are unknown. EmrA was shown to form both dimers and

54   trimers [12] and electron microscopy data of reconstituted EmrAB suggests a putative 'dimer

55   of dimers' assembly [13]. Arrows indicate energy-coupling (brown) and the proposed

56   schematic substrate transport pathways (black). LPS abbreviates lipopolysaccharide, and the

57   peptidoglycan is composed of repeating units of the disaccharide N-acetyl glucosamine-N-

58   acetyl muramic acid.

59

60   Tripartite systems play numerous physiological roles beyond capacity for antibiotic

61   efflux, as might be anticipated from their ancient evolutionary history. For example, some of

62   the pumps can transport quorum signalling molecules [14-17] and virulence factors [18-27], or

63   act as a "metabolic relief valve" to expel products that become hazardous due to imbalanced

64   metabolism [28].

65   Atomistic structures of the individual components and the full assemblies have been

66   elucidated for the RND and ATP-based pumps, and we describe here the key features of the

67   quaternary organisation and the communication between subunits during the transport process.

68

69   **The components of tripartite efflux pumps**

70   Three protein components form the canonical tripartite assembly. The individual

71   component structures of the AcrAB-TolC tripartite pump assembly, including the auxiliary

72   factor AcrZ, are displayed in Figure 2. We present each of the components in turn.

73   The inner membrane protein component (IMP) of the pump assembly, i.e. the

74   transporter, transduces energy to drive the active efflux of substrates through the tripartite

75   assembly. The inner membrane ATP-binding cassette transporters such as MacB of the

76   MacAB-TolC tripartite system couple transport processes with the binding and hydrolysis of

77   ATP. AcrB and other RND transporters harness the energy from the controlled flow of protons

78   to promote conformational changes that enable binding and movement of substrates into the

79   channel of tripartite assembly. Structures of AcrB [29] in apo and ligand-bound states have

80   been solved using X-ray crystallography and provide insight into the conformational changes

81   associated with substrate binding and the pathway for conducting protons. AcrB has a peptide

82   partner AcrZ that affects its transport activity for a subset of substrates. AcrZ is a small protein

83   of 49 amino acids that makes an extensive interface with the AcrB transmembrane domain

84   [30].

85   TolC is a representative of the outer membrane protein (OMP) component of tripartite

86   pump (Figure 2A, B). Crystal structures of TolC from numerous species, including *E. coli* and

87   the homologue VceC from *Vibrio cholerae*, reveal an architecture of extended α-helices that

88   bundle into coiled-coils and pinch together to form a semi-porous seal at the periplasmic end

89   of the trimer. At the time that the first crystal structure of the isolated TolC was elucidated, it

90   seemed clear that the closed periplasmic end must be dilated at some stage of the transport

91   process in order to accommodate even the smallest of the known transport substrates. The

92   process of TolC opening has now been visualised from the high-resolution structures of the

93   tripartite efflux pumps that will be described later in this chapter.

94   The periplasmic component of the tripartite architecture, the membrane fusion protein

95   (MFP), bridges the IMP and the OMP. This protein class is characterised by defined domains

96   identified by high resolution crystal structures, namely – the α-helical hairpin, lipoyl-like, β-

97   barrel and membrane proximal domains (Figure 2A, C). As we will describe below in detail,

98   the MFP allosterically transduces conformational change from IMP to OMP.

99

100
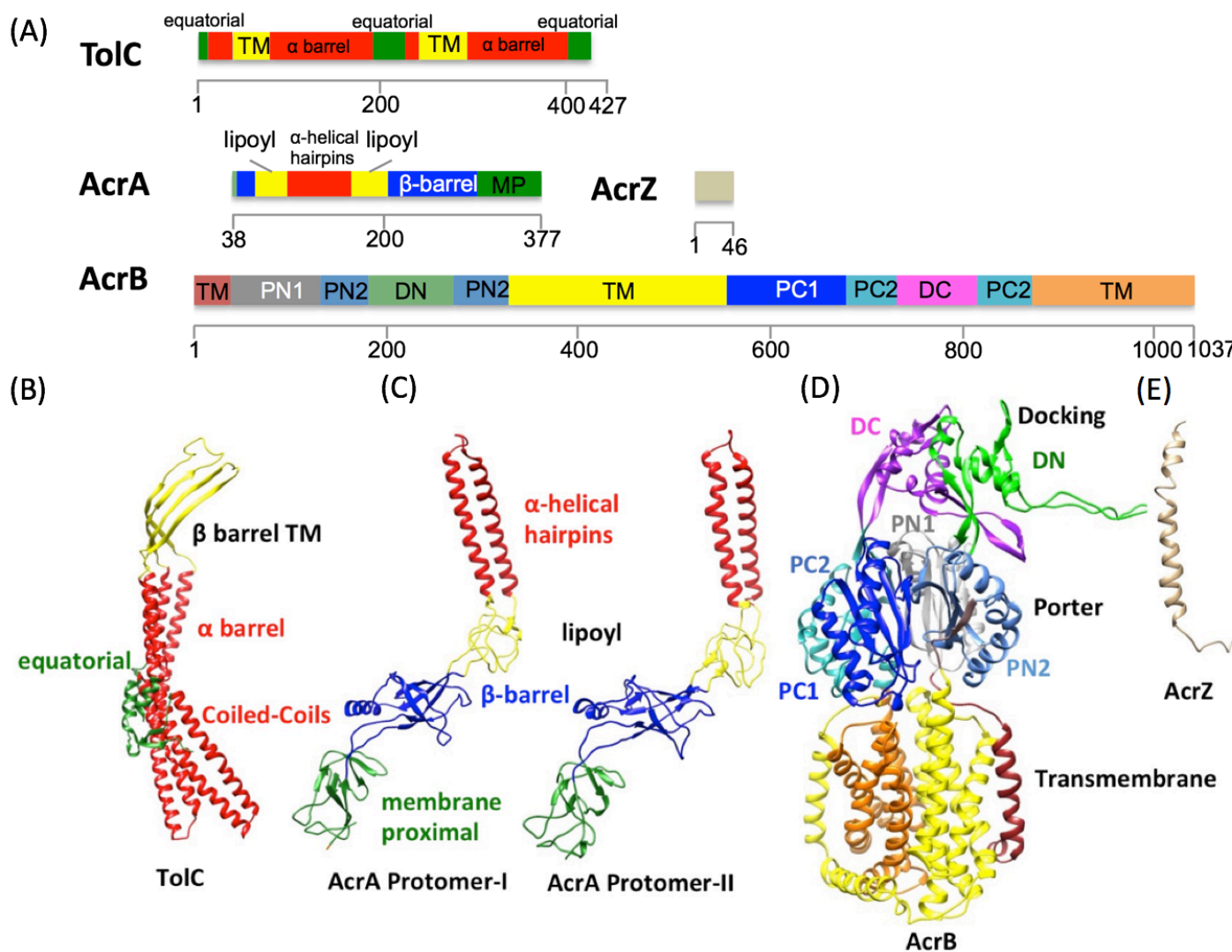
101

102   **Fig. 2. A structural gallery of the AcrAB-TolC pump components and their domains.** (A)

103   Linear representation of the protein components of the AcrABZ-TolC system. (B-E) Protomer

104   structures of the tripartite efflux pump components: TolC (B), AcrA Protomer-I and -II (C),

105   AcrB (D), and AcrZ (E). TolC and AcrB form stable homotrimers in isolation, and both

106   proteins have an internal structural repeat that arose from an ancestral gene duplication event.

107   The figure was adapted from [31].

108

Architecture of the tripartite pumps

110   Combining the advances in electron cryo-microscopy (cryo-EM) with novel

111   engineering approaches to stabilise the tripartite efflux pump assemblies, high-resolution

112   structures have been attained for AcrAB-TolC [31, 32] and MacAB-TolC [33]. The cryo-EM

113   structures of AcrAB-TolC reveal a trimer of TolC, a trimer of AcrB, and a hexamer of AcrA

114   that bridges the two membrane protein components [31]. Some biochemical and genetic

115   experiments indicate that only 3 molecules of AcrA (instead of 6) are sufficient for AcrAB-

116   TolC activity [34, 35], but this would not allow formation of a complex that is sealed so that

117   substrates do not flow into the periplasm. The MacAB-TolC has a similar architecture to

118   AcrAB-TolC, with a trimer of TolC and a hexamer of the periplasmic partner MacA; however,

119   the inner membrane ATPase transporter MacB is a dimer [33, 36-39], in contrast to the trimeric

120   AcrB transporter. For both systems, TolC interacts directly with the periplasmic partner (AcrA

121   or MacA) in similar manner. On the other hand, there are no apparent similarities in the

122   interactions of the trimeric AcrB with AcrA or the dimeric MacB with MacA. The atomic

123   models of the AcrAB-TolC and MacAB-TolC tripartite assemblies are shown in Figure 3.

124
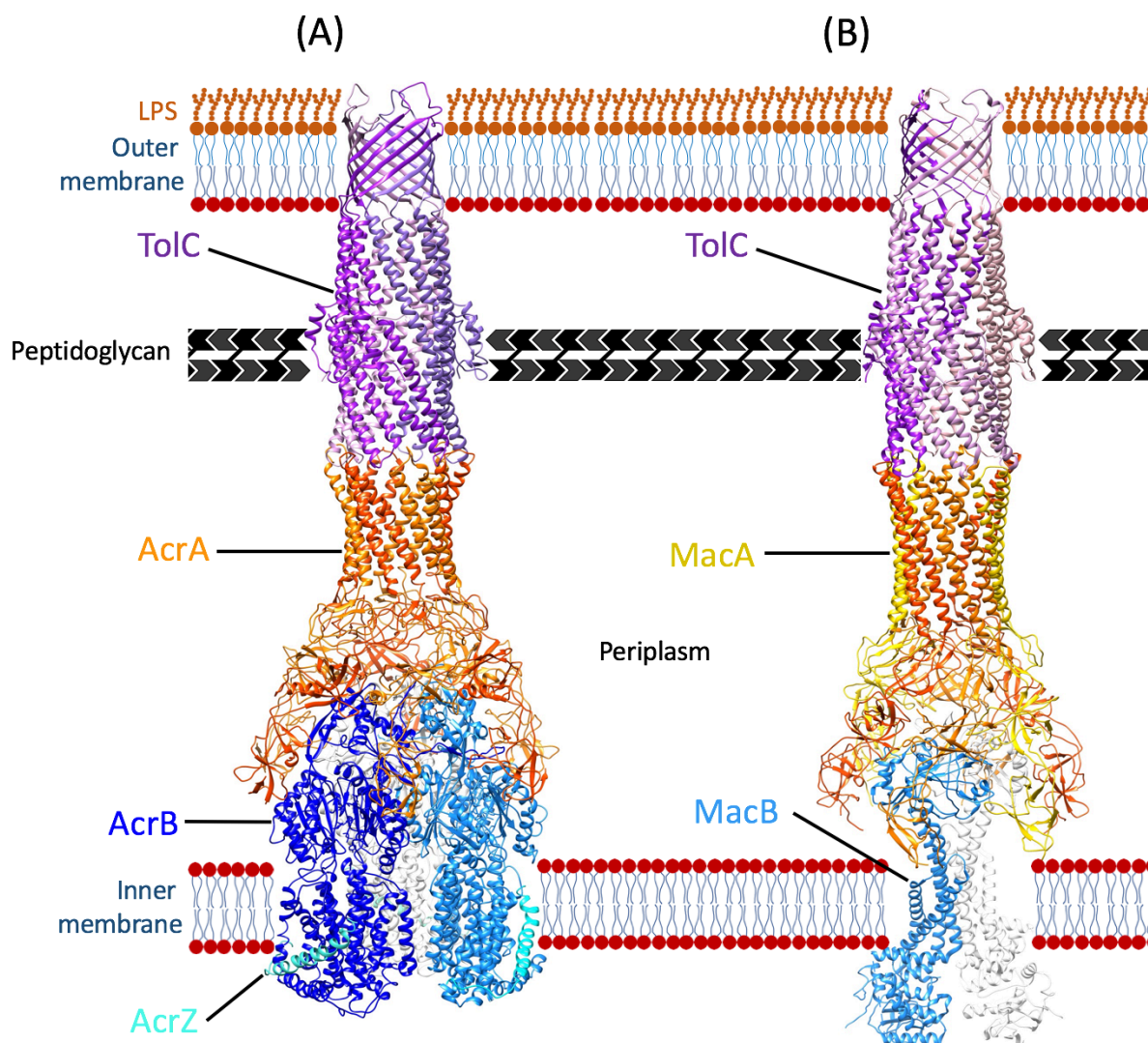
Fig. 3. Models of two tripartite assemblies, with speculation of the position of the peptidoglycan layer. (A) Structure of the RND-based AcrABZ-TolC (adapted after [31]), with a TolC trimer, an AcrA hexamer and AcrBZ trimer. (B) Structure the ABC-based MacAB-TolC (adapted after [33]), with the TolC trimer, MacA hexamer and MacB dimer. TolC could potentially be anchored by an interaction between the equatorial domain and the peptidoglycan matrix in the periplasm. The speculation interaction of TolC with the peptidoglycan is based on the location of the layer based on tomographic reconstructions [40].

Although TolC and AcrB are both homo-trimers, the periplasmic partners MacA and AcrA are hexamers, and consequently the interactions between these proteins must involve a

136 loss of symmetry. The latter was evident from crystallographic data of AcrB captured with

137 each of the three protomers in a different conformational state [41-43]. In fact, TolC and AcrB

138 both bear a structural repeat and are therefore 'honorary' hexamers. Thus, the six interaction

139 interfaces made between AcrA and either TolC or AcrB are approximately but not exactly

140 equivalent. The same is true for the six interaction interfaces made between MacA and TolC.

141 To distinguish these interfaces, the protomers in Figure 4A of AcrA are labelled as protomers

142 I and II. The helix-turn-helix (HTH) elements at the periplasmic end of TolC interact in a tip-

143 to-tip fashion with the HTH units in the α-helical hairpin domains of AcrA [31] (i.e., six HTH

144 units of the AcrA hexamer interact with 3 x 2 HTH units of the TolC trimer) (Fig. 4(B)). In

145 detail, the AcrA protomer-I/TolC alignment involves residues K140 and S139 of AcrA and

146 G365 of TolC [32] (Fig. 4(C)). Furthermore, L132 of AcrA is in direct contact with N145 and

147 T366 of TolC [31].

148   In the AcrAB-TolC pump, each of the three AcrA protomers-I aligns with the DN and

149 DC subdomains of one AcrB protomer via its β-barrel domain, whereas its MP domain interacts

150 with the PC1 subdomain, the PC2-DC linker-region, and a DN subdomain loop of a

151 neighbouring AcrB protomer [31, 44] (Fig. 4(A)). AcrA protomer-II interacts with a β-hairpin

152 of one AcrB protomer and a short α-helix of the DC subdomain of an adjacent AcrB protomer

153 [31, 44] (Fig. 4(A)). The β-hairpin motif in the DN subdomain of AcrB was shown to be crucial

154 for correct assembly of an active pump complex [45].

155   Both apo- and ligand-bound states of the AcrAB-TolC pump have been elucidated by

156 cryo-EM [35]. In the apo-form state, the TolC trimer resembles the closed state seen in the

157 crystal structure of the isolated protein, which has a constriction point where the coiled coils

158 pinch together. In this closed state, inter-protomer hydrogen bonds are made between residue

159 R367 of one protomer and T152, D153 and Y362 of an adjacent protomer [46-48]. However,

160 for the ligand-bound structures of the pump, TolC is in an open state. Comparing the open and

161 closed forms suggests that TolC opens up in an iris-like dilation at its periplasmic end [31]

162 through changes in the coiled coil geometry mediated through interaction with AcrA [49] (Fig.

163 4(D)). In the MacAB-TolC assembly, the TolC is also in an open state. Six glutamine residues

164 in the loops of MacA lipoyl domains form a uni-directional valve, which probably prevents

165 back leakage of substrate into the periplasm during transport [33]. A direct interaction of

166 substrate with the MFP may also occur for type-1 secretion systems [50].

167
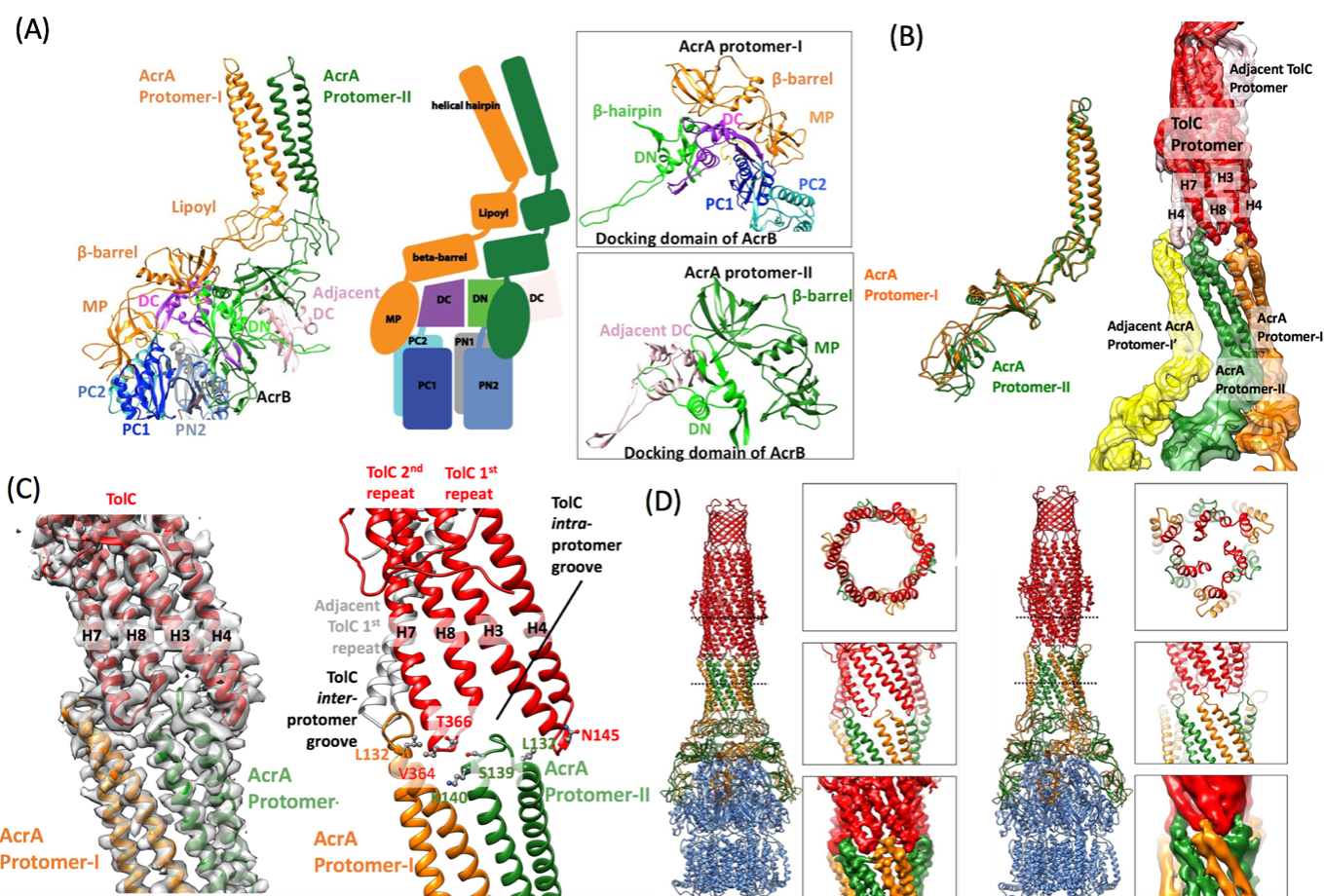
168

169 **Fig. 4. Overview of interactions between the AcrAB-TolC tripartite pump components.**

170 (A) Interaction of AcrA protomers I and II with subdomains PC1/2, PN1/2, and DC/DN of

171 AcrB. (B) Cryo-EM map with fitted model shows the tip-to-tip interactions between AcrA and

172 TolC in the resting state of the pump. (C) The tip-to-tip alignment of HTH motifs between

173   TolC and AcrA in the transport state. (D) The resting and transport state of TolC. Figure panels

174   (A-D) adapted after [31].

175

Conformational states and allosteric coupling in the AcrAB-TolC tripartite assembly

177   Crystallographic data suggest that AcrB transitions through three distinct

178   conformational states during the transport process, referred to as 'loose', 'tight', and 'open'

179   (Fig 5) [31, 41-43]. In this mechanism, a substrate enters ('Access', or 'L' for loose) through a

180   peripheral cleft and binds ('Binding', or 'T' for tight) to the drug-binding pocket of AcrB. The

181   peripheral cleft closes up and a second pathway is opened ('Extrusion', or 'O' for open)

182   towards the funnel in the docking domain of AcrB − through which the substrate eventually

183   enters the AcrA-TolC 'pipeline' for extrusion to the cell's exterior (Fig 5 A, B) [31, 41, 51].

184

185
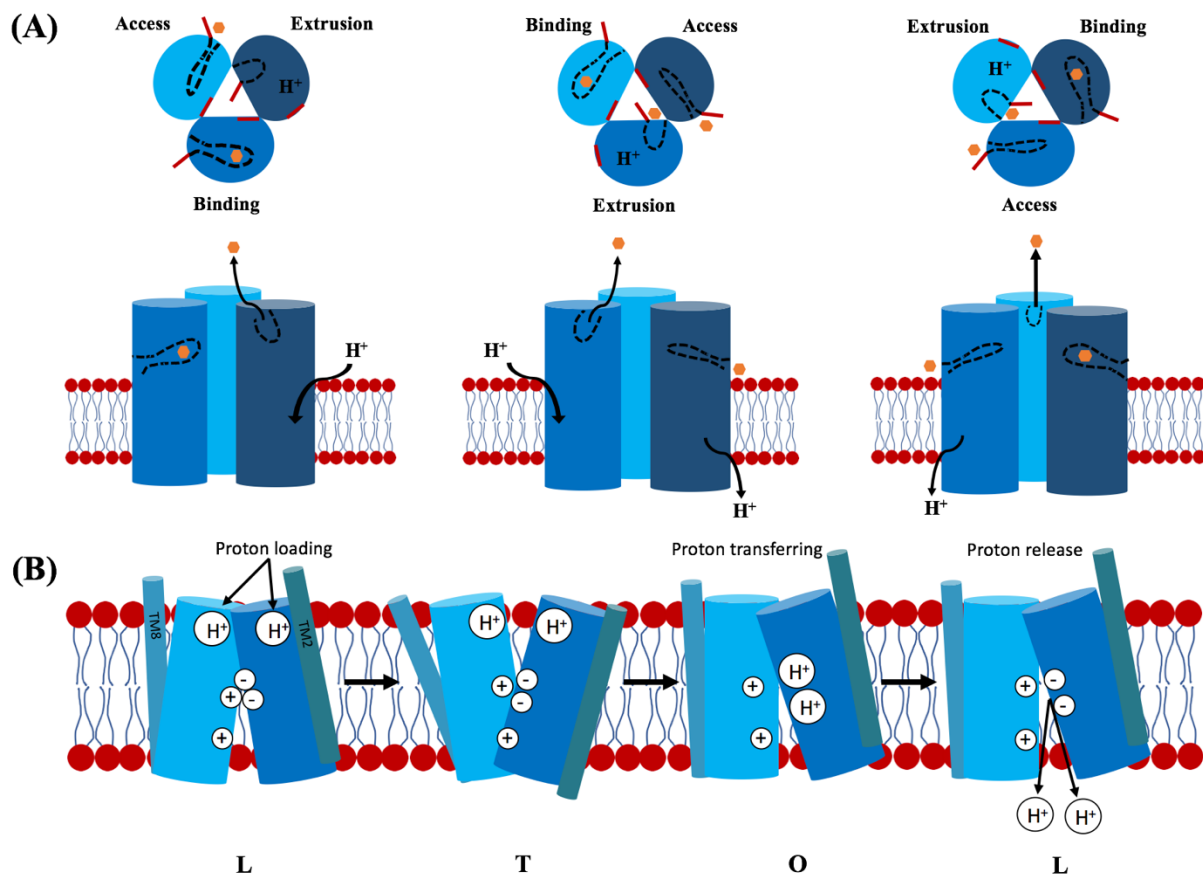
186 **Fig. 5**. **Cartoon schematic of the transport mechanism for AcrB.** (A) The proposed ordered

187 steps in binding of transport substrates (adapted after [52]). The orange circle represents the

188 transport substrate, and the H^+ is associated with titratable residues in the protein. (B) Energy

189 transmission and upward movement of TM2 towards the AcrB periplasmic pore domain in

190 response to protonation events in the trans-membrane domain for drug translocation [53,

191 54].

192

193   Transport substrates enter the AcrB-protomers via the pore domain formed by the

194 PN1/PN2 and PC1/PC2 subdomains (Fig. 4A and Fig. 2D) [29, 41]. The PN1/PN2 subdomains

195 extend into the periplasm between TM1 and TM2, while PC1/PC2 are located between TM7

196 and TM8 [29, 41]. All four subdomains together form an access (or proximal) pocket and a

197 deep binding (or distal) pocket of an AcrB protomer [29, 41]. Differences between these two

198 pockets in aromatic, charged, and polar residues are suggested to affect substrate preferences

199 [55]. Water molecules have been found to additionally stabilize substrate binding [51, 56]

200 inside the pocket and to contribute to drug binding and transport [57].

201   Substrates from the periplasm are thought to enter through a cleft formed by PC1/ PC2

202 subdomains (Channel 1; Fig. 6) [51, 58]. Channel 1 seems to be present in both L and T

203 protomers with the PC1/PC2 cleft being more closed in T. Substrates from the outer leaflet of

204 the inner membrane are thought to gain access via two grooves formed between trans-

205 membrane helices 1 (TM1) and 2 (TM2) or TM7 and TM8, respectively (Channel 2; Fig. 6)

206 [53]. High molecular weight macrolides (and maybe other substrates) are thought to enter via

207 this channel.

208   A third channel for drug entry (Fig. 6), with preference for planar, cationic aromatic

209 compounds of low molecular mass (such as ethidium), has been hypothesised to take up

210 substrate from a vestibule of an inner cavity formed between the three AcrB protomers [59].

211 The third channel therefore by-passes the proximal binding pocket and the switch-loop that

212 separates the two binding pockets (in red;) [59].

213 There might be additional channels in AcrB given that carboxylated drugs (e.g. β-

214 lactams) were found to bind to the groove between TM1/TM2 [53]. One difficulty with these

215 suggested binding sites is that they are relatively far from both binding pockets. However, a

216 recently solved crystal structure of AcrB with fusidic acid bound in a cavity formed between

217 TM1 and TM2 suggests that an upward movement of TM2 towards the AcrB periplasmic

218 pore domain in response to protonation events in the transmembrane domain might help to

219 translocate the drugs further into the assembly towards the AcrA-TolC tunnel [53] (Fig. 5B).

220
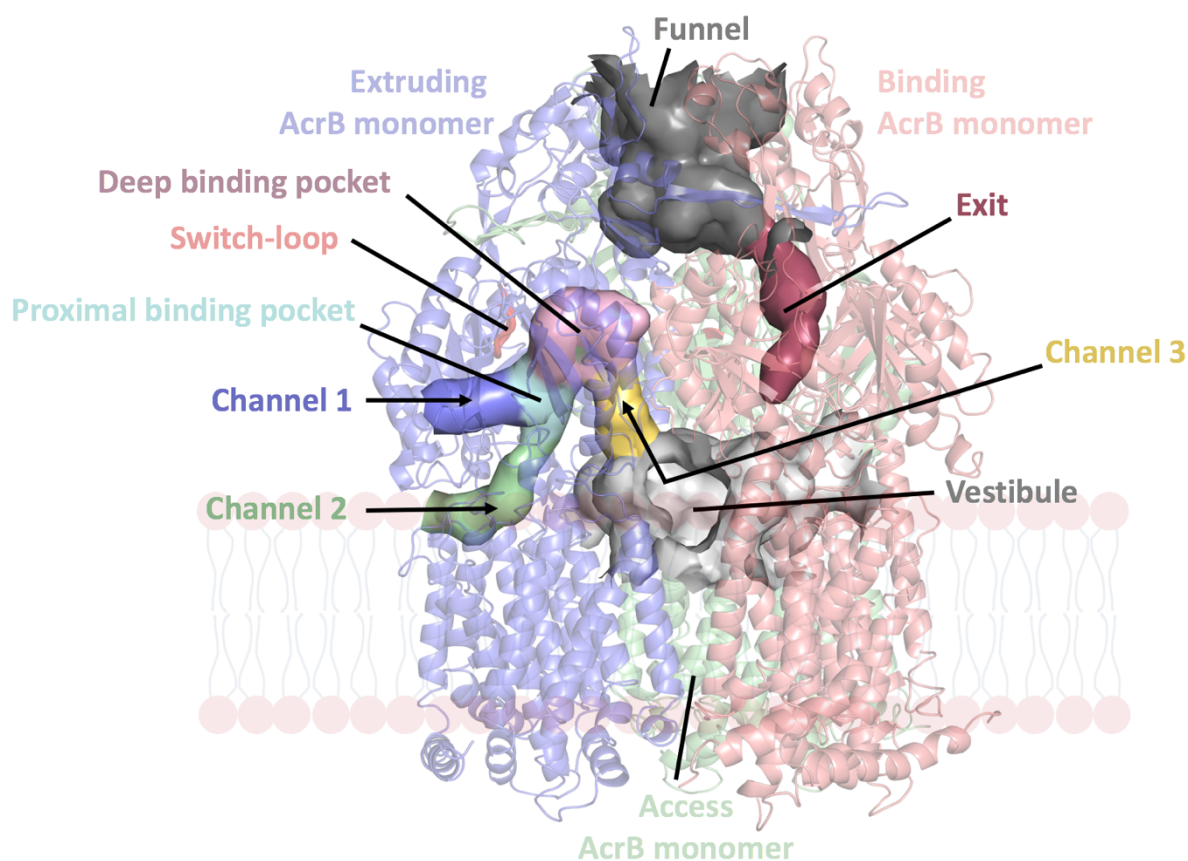
221

222 **Fig. 6. The three channels proposed for substrate entry in AcrB.** Substrates can enter AcrB

223 from the periplasm (Channel 1, purple) or from the outer leaflet of the inner membrane

224 (Channel 2, green). Both lead via a proximal binding pocket (light blue) to a deep binding

225   pocket (pink). The third channel (Channel 3, yellow) is directly connected with the deep

226   binding pocket and has its entrance from a central vestibule in a central cavity formed between

227   the three AcrB protomers. It therefore by-passes the proximal binding pocket and switch-loop.

228   All substrates leave the AcrB protomer via an exit channel (dark red). The latter leads to the

229   funnel from which the substrate then passes through the AcrA-TolC tunnel with facilitation by

230   water molecules [57].

231

232   Large conformational changes are observed in AcrB's PN1/PC2 and PN2/PC1 modules

233   during cycling through the L, T, and O states [51, 54], and the PN2/PC1 module opens and

234   closes the deep binding pocket. The cycling through the three distinct conformational states

235   appears to progress in a defined pattern, and the mechanism has accordingly often been referred

236   to as "peristaltic" [42]. However, a recent investigation of crystal structures in combination

237   with functional studies of the trimeric CemB, a AcrB homologue from the Gram-negative

238   pathogen *Campylobacter jejuni*, suggests that CemB's protomers perform conformational

239   cycling independently from each other during the efflux process [60]. In the absence of a proton

240   gradient, the protomers enter a symmetric resting state. It is not clear yet whether this model is

241   distinct for a certain class of AcrB homologues, or applies more broadly and challenges the

242   current model of ordered and coordinated transitions between distinct states.

243   The cryo-EM data of AcrAB-TolC in the presence of puromycin identify different

244   conformational states of AcrB in the full pump assembly which are consistent with the findings

245   described above from X-ray crystallography [41, 42]. In the apo-state (resting state) of the

246   pump, all three AcrB sub-units are in 'loose' conformation and TolC is in a closed state in

247   which the channel is occluded for substrate exit. In this state, the AcrA subunits pack in manner

248   that leaves gaps between the α-helical hairpin, lipoyl, and β-barrel domains. However, with

249   transition to the ligand-bound form (transport state), the AcrA subunits re-pack to seal the gaps.

250   The configuration of the AcrA hexamer in the ligand-bound form opens the periplasmic end of

251   TolC by tip-to-tip interactions of helical hairpins (Fig. 4(C, D)). The movement of AcrA that

252   occurs with the apo- to ligand transition is inferred to originate from an energy-derived

253   conformational switch in AcrB [31, 32]. A potential energy-conveying communication

254   between the MFP and inner membrane components is also illustrated by the MacAB-TolC

255   system, for which it was shown that MacA stimulates the ATPase activity of MacB [61]. The

256   transition from resting to transport state of AcrAB-TolC is associated with a contraction of the

257   pump along the long axis by ca. 10 Å. This contraction must result in a local compression of

258   the periplasm to accommodate the axial contraction of the pump as well as a change in

259   curvature of the outer and inner membrane near AcrB's portal [31].

260

261   **Substrate interactions and substrate pathway**

262   Whereas substrate binding and the internal translocation mechanism is well explored

263   for AcrB, for most other identified transporters it is not clear how the inner membrane

264   component of the tripartite assembly interacts with the substrate. Three different entry routes

265   of the substrate into the transporter are possible in principle: One from the inner or outer leaflet

266   of the inner membrane, another from the cytoplasm, and the last from the periplasm. A

267   substrate transported across the inner membrane into the periplasm by a 'stand-alone'

268   transporter like MsbA may be picked up by a tripartite system and expelled across the outer

269   membrane through the complex assembly. Indeed, there are dozens of different transport

270   systems typically expressed simultaneously in a single bacterial cell, of which some work in a

271   stand-alone manner as inner membrane transporters, and they can work in conjunction with

272   tripartite assemblies as part of an efflux super-system [62-64] .

273   The tripartite AcrAB-TolC system has been shown to transport chemically diverse

274   substrates, including antibiotics like chloramphenicol, tetracycline, novobiocin, fusidic,

275 nalidixic acid, fluoroquinolones, various members of the β-lactam and macrolide antibiotic

276 families [5, 6], as well as Triton X-100, bile salts, cationic dyes, disinfectants [7], nonpolar

277 solvents [8, 9] and the mammalian steroid hormones estradiol and progesterone [65]. In the

278 case of the *E. coli* MacAB-TolC system*,* transported substrates include macrolide [66],

279 glycolipid [67], and lipopeptide [68], as well as the heat-stable enterotoxin II [69] which forms

280 pores in mucosal cells of the intestinal wall.

281 It is yet to be fully understood how the enormous poly-specificity of multidrug efflux

282 tripartite assemblies arises. In part, the poly-specificity may arise from multiple binding sites

283 residing within the same or different substrate binding pocket(s) [51, 58, 70, 71]. A puromycin-

284 bound AcrB structure provides an illustrating example for the complexity behind the significant

285 poly-specificity observed in many transporters (Fig. 7). Some useful parallels may be drawn to

286 QacR, a drug-binding regulator (repressor) of *qacA* (a MFS multidrug pump encoding gene

287 from *Staphylococcus aureus*) [72, 73] for which multiple, linked drug-binding sites were

288 identified [74]. For the mammalian ABC transporter ABCB1, data suggest the existence of

289 multiple drug-binding pockets [75].

290

291

292
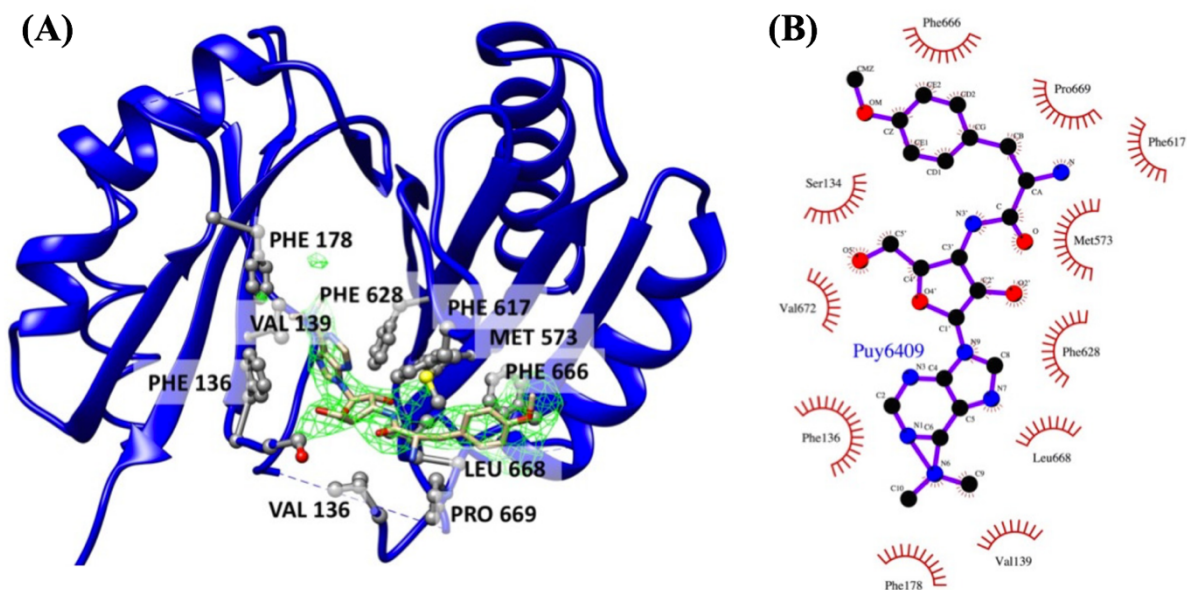
Fig. 7. Puromycin-bound AcrB structure. (A) The antibiotic is bound in the deep binding pocket of AcrB. (B) Schematic overview of main contacts between puromycin and AcrB. Figure adapted after [31] (PDB ID 5NC5).

MacB and Type I Secretion System ABC transporters

Tripartite efflux pump systems are closely related to the multi-component type I secretion machineries involved in the export of virulence proteins. For instance, the membrane fusion components share a similar binding motif for the outer membrane channel TolC [76]. The recently solved structures of the inner membrane ABC transporter component of a type I secretion system (*Aquifex aeolicus* AaPrtD, part of AaPrtDEF assembly) [77] and that of the ABC transporter MacB from the tripartite multi-drug efflux assembly MacAB-TolC [33, 37-39] invite a structural comparison of these two systems. Both structures are depicted in Fig. 8.
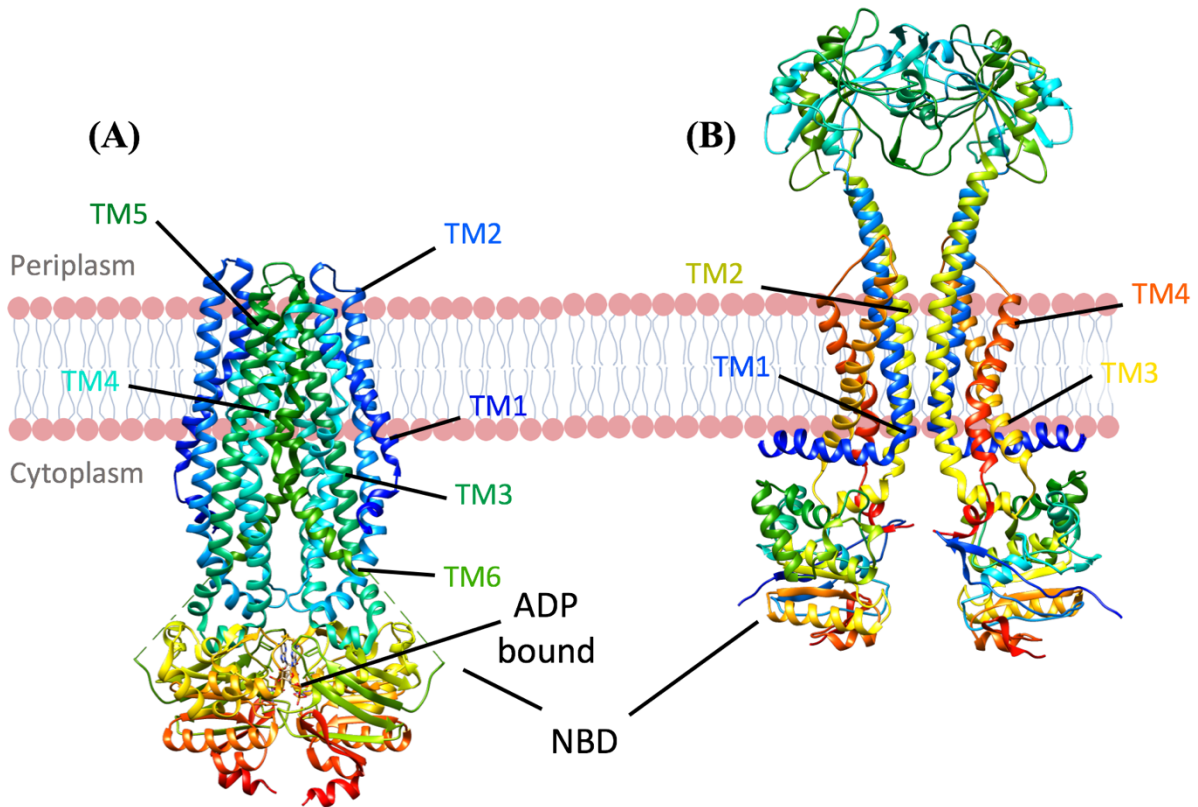
Fig. 8. Structural comparison between two ABC transporter components of tripartite assemblies. (A) AaPrtD, the *Aquifex aeolicus* ABC transporter of the type 1 secretion system with close overall resemblance to many other solved ABC transporters (adapted after [77]). (B) MacB, the ABC transporter of the MacAB-TolC multi-drug efflux pump with its characteristic periplasmic domains (unique to all so far solved ABC transporters). The periplasmic domain forms extensive interactions with MacA in the tripartite assembly. The figure was adapted from [33].

For most homo-dimeric ABC transporters, a transport model has been proposed according to which substrate engages a binding pocket in an inward-open state and is then expelled to the opposite site of the membrane when ATP-binding initiates a conformational change towards the outward-open state [78-85]. This alternating access model [80] is supported by observations from crystal structure of various ABC transporters that are captured in inward-facing and outward-facing conformations [71, 79, 81, 82, 86-89]. The alternating access model

320   is summarised in Fig. 9(A)), depicting two identical protomers performing a clothes peg-like

321   movement in a two-state cycle [85, 90]. According to this model, substrate enters the binding

322   pocket(s) (several binding sites have been suggested for ABCB1, see [75, 91]) of the

323   transporter in its inward-facing conformation. Substrate can access the transporter from the

324   cytoplasm or the directly from the inner leaflet of the inner membrane (likely to be the case for

325   hydrophobic substrates).

326   The mechanism is depicted schematically in Fig. 9. A transporter with ATP bound to

327   both nucleotide-binding domains (NBDs) undergoes conformational sampling, which enables

328   NBD dimerization when a substrate binds [85]. An intermediate state occurs that has an

329   occluded ATP in one nucleotide-binding site (NBS1) and a loose ATP in NBS2. The occluded

330   ATP at NBS1 is hydrolysed to ADP-P_i whereas the loose ATP in NBS2 becomes occluded

331   [85]. The hydrolysis of the occluded ATP in NBS2 to ADP-P_i drives a conformational switch

332   to an outward-open conformation (like pressing the clothes pegs together); also, the inorganic

333   phosphate dissociates from the ADP in NBS1 and the occluded ATP in NBS2 is hydrolysed to

334   ADP-P_i [85]. In the outward-open conformation, substrate is released into the outer leaflet of

335   the membrane [85].

336   For hetero-dimeric ABC transporters, a constant-contact model (not displayed here) has

337   been suggested, in which the NBDs never fully detach from each other [90, 92]. Here, substrate

338   binds whilst one ATP molecule keeps the protomers together (i.e. catalytic asymmetry between

339   NBDs) [90, 93-95]. A second ATP then binds and is hydrolysed – as a result of which

340   protomers adapt another asymmetric state and substrate is released to the outside [90].

341   Following substrate release and the dissociation of phosphate, the protomers re-adapt the apo-

342   state with one ATP molecule still holding both halves together [90]. The release of ADP

343   enables re-binding of substrate [90].

It is therefore plausible that homo-dimeric transporters also cycle through step-wise ATPase stages, instead of both ATP molecules being hydrolysed simultaneously. Interestingly, a constant-contact with catalytic asymmetry has also been suggested for the mammalian homo-dimeric ABC transporter P-glycoprotein [96-98].
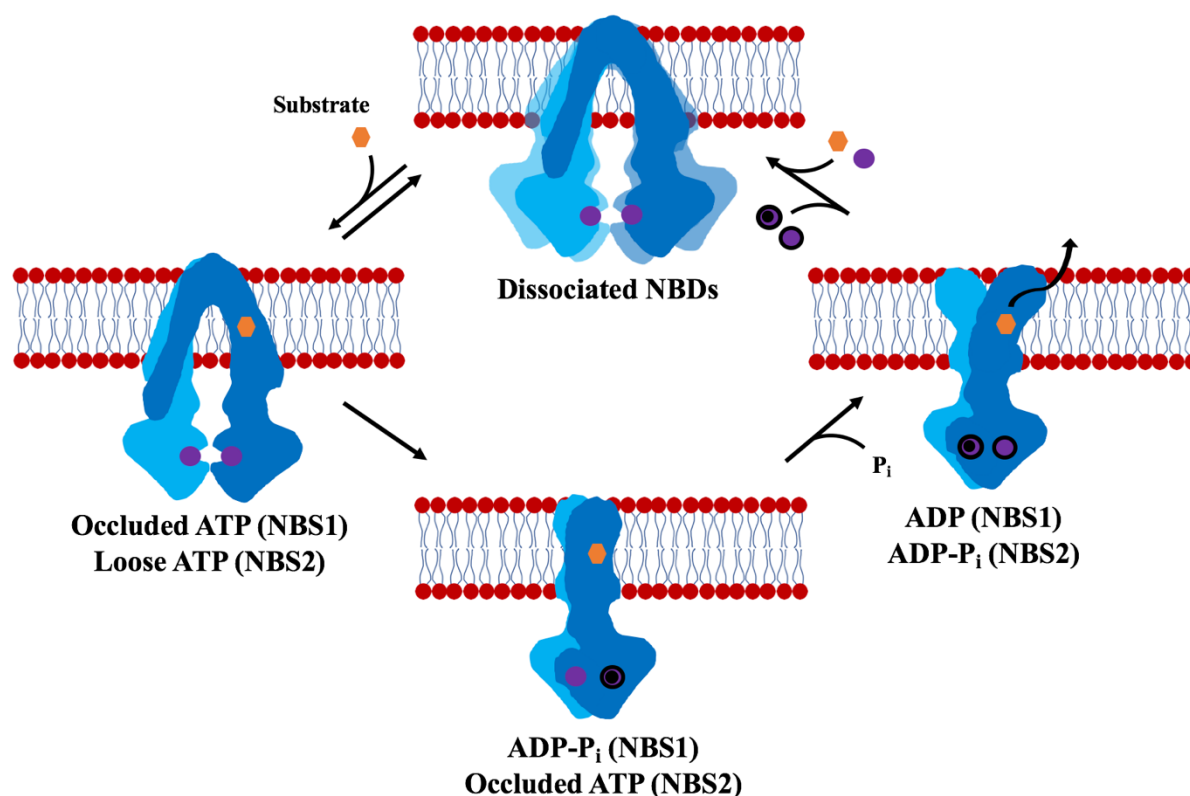
Fig. 9. Alternating access model for ABC transporter. Blue figures, two half-transporters; purple circles, ATP; purple circles with black borders, ADP; purple circles with black borders and black central dot, ADP-P_i; orange hexagon, drug/substrate. In the outward-open (pressed drying clothes peg-like) conformations, the trans-membrane domains of the transporters are opened up towards the external side of the membrane. Each depicted domain wing contains two trans-membrane helices: From one trans-membrane domain and four trans-membrane helices from the other half. Model adapted after [85].

358   Like MacB, the *Aquifex aeolicus* PrtD protein (aaPrtD) forms a homo-dimer (Figure 8).

359   aaPrtD is the energy transducing component of a tripartite Type I secretion system that includes

360   the MFP PrtE, and the OMP PrtF. Type I secretion complexes transport virulence factors,

361   including ligases, scavenging molecules, and proteases [99-102]. These transport substrates

362   must be in an unfolded state in order to be transported [103, 104]. Interestingly, with some of

363   these substrates exceeding 8,000 amino acids [99, 101], these lengthy unfolded polypeptide

364   chains are assumed to move continuously through a pore formed by the transmembrane

365   domains [105, 106]. A well-studied Type I section system is the HlyDB-TolC complex that

366   transports hemolysin A (HlyA), for which experimental evidence indicates transport occurs

367   directly from the cytosol without a periplasmic intermediate [99, 107-109]. In the case of PrtD,

368   a basal ATPase activity may be repressed by substrate binding, which could prevent the closure

369   of nucleotide-binding domains. In this state, PrtD binds the other components PrtE and PrtF

370   [77, 110-112]. The full assembly is suggested to reactivate PrtD's ATPase activity and

371   therewith to enable the substrate transport [77, 113, 114]. A potentially related stimulation by

372   the MFP has previously been demonstrated for the interaction of MacA with MacB [61]. How

373   ABC transporters like PrtD transport peptides requires further characterization.

374   Although MacB was originally described as a macrolide efflux inner membrane

375   transporter as part of the MacAB-TolC tripartite system, it has been shown to also transport a

376   71 amino-acid long heat-stable enterotoxin II (STb-II) [69]. Unlike the Type I secretion system,

377   the peptide substrate appears to be taken up by the MacAB-TolC tripartite machinery from the

378   periplasm rather than the cytoplasm, since the STb-II is translocated via the Sec system into

379   the periplasm where it is processed [115-117]. This periplasmic entry could hint towards an

380   alternative transport mechanism to those observed for other ABC transporters so far. In this

381   model, substrate enters MacB via the periplasm and binds to a disclosed binding cavity in the

382   outward-open MacB-dimer, while ATP hydrolysis and release of inorganic phosphate might

383   then trigger the release of substrate with subsequent passage through MacA into the MacA-

384   TolC part of the extrusion machinery. This resembles more closely the outward-only model as

385   distinct from the alternating access model.

386   In comparison to AaPrtD and all other structurally characterised ABC transporters,

387   MacB has extensive periplasmic domains. The MacB periplasmic domains form interactions

388   with MacA, and since these are not present in AaPrtD, the Type I secretion systems must have

389   a different organization for the interactions between the ABC and MFP components. MacB

390   reveals the characteristic 'anchoring' helices at the inner leaflet-cytosol interface [33, 37-39]

391   which so far have been observed in an ABCG5/8 type-II exporter structure [118]. MacB

392   furthermore shows closer proximity of nucleotide-binding domains to the inner leaflet, as

393   opposed to the larger extensions of trans-membrane (TM) helices into the cytosol in other ABC

394   transporters. MacB's 4 trans-membrane helices lack the characteristic kinks seen in AaPrtD's

395   TM3 and TM6 [77], and the 4 TMs are the smallest observed number amongst ABC

396   transporters with known structures [119]. AaPrtD utilises both pairs of its 6-bundled TMs to

397   form a continuous channel for unfolded substrate transport across the inner membrane, which

398   in the resolved ADP-bound occluded structure was closed at the cytosolic side via a conserved

399   Arginine on TM6 between TM6 and TM4, and on the periplasmic side via a pore ring

400   consisting of hydrophobic residues [77]. The latter is unique amongst known transporters and

401   may prevent leakage of protons along the gradient [77].

402   The location of the substrate binding site(s) is unknown for both transporters. For

403   AaPrtD, substrate interaction at the concave surface and near the cytosolic window where TM4

404   separates from TM6 have been suggested [77] based on previous studies [105, 120-123]. For

405   MacB, an unidentified density, occluding the region between the periplasmic extensions of

406   TM1 and TM2, might hint towards a putative substrate interaction or binding site [33].

407

408 **Tripartite pump regulation**

409   Analyses of overexpressed tripartite pumps involved in the efflux of multiple antibiotic

410 compounds in clinical isolates [124, 125] demonstrate the importance of pump regulation for

411 drug design applications and clinical practice. Tripartite pump expression levels can be

412 regulated by two component systems comprised of a sensor histidine kinase and a response

413 regulator (the mechanisms of two component systems are reviewed in [126-128] *inter alia*).

414 Mutations in these systems have been identified in numerous clinical isolates [129] and were

415 shown to contribute to pump overexpression [129-131]. In brief, first a histidine kinase senses

416 environmental signals like the presence of toxic compounds (e.g. antibiotics). The 'sensing'

417 usually happens indirectly though cases of direct sensing are known: The *Streptomyces*

418 *coelicolor* VanS (VanSsc) histidine kinase was shown to directly bind vancomycin [132].

419 Interestingly, in the case of bacitracin resistance in *Bacillus subtilis*, the bacitracin transporting

420 ABC transporter BceAB acts as a sensor itself by mediating information on its transport

421 activity, though protein-protein interaction, to the histidine kinase BceS [133]. Other examples

422 for two component systems that regulate efflux pump expression include AmgRS in

423 *Pseudomonas aeruginosa*, CpxAR in *Enterobacteriaceae*, and AdeSR in *Acinetobacter*

424 *baumannii* [134]. In the latter case, AdeR (the response regulator) activates the expression of

425 the *adeABC* tripartite system genes by binding to a direct-repeat motif in the intercistronic

426 spacer [135]. Interestingly, at least some two component systems seem to be capable of multi-

427 system regulation: The BaeSR system in *Salmonella typhimurium*, for instance, has been

428 shown to regulate both *acrD* and *mdtABC* expression [136]. The same system in *E. coli*

429 activates both of the latter in response to the presence of indole [137].

430   Further along the signal transduction cascade, local and global regulators fine-tune

431 tripartite system expression levels. For instance, transcription of *acrAB*, encoding AcrA and

432 AcrB is controlled by local repressors like AcrR [138], global regulators like MarA, SoxS,

433   and Rob [139], as well as global expression activators like RamA [140, 141] (with its

434   repressor protein RamR [142], whose RamA-repressing activity in turn is downregulated

435   via drug binding [143]). Other local repressors like TetR/QacR family members (e.g. *emrR*,

436   *acrR*, *mtrR*) downregulate pump expression [144-147]. These control elements reveal a rather

437   complex regulatory network for fine-tuned expression. Overexpression of AraC/XylS global

438   regulator family members (e.g. MarA, SoxS, and Rob) has been shown to result in pump

439   overexpression and consequently increased efflux activity [148]. These regulators can be

440   induced by substrates of the pump systems they are regulating. In *Pseudomonas aeruginosa*,

441   for example, the *mexZ* gene encodes a putative repressor of the *mexYX* operon (part of the

442   MexXY-OprM tripartite system). In a *mexZ*-defective mutant, the *mexY* gene was found to be

443   induced by various ribosome inhibitors like macrolides and chloramphenicol, but not by

444   antibiotics acting on other cellular targets [149]. Such a complex regulatory pattern hints

445   towards an additional physiological role for the Mex system beyond antibiotic efflux, and

446   suggests that there are additional regulatory loci for *mexYX* [149]. Surprisingly, for the MexEF-

447   OprN tripartite pump in *P. aeruginosa*, toxic electrophiles were recently identified to induce

448   expression through the transcriptional regulator CmrA [150].

449   Regulation of different pump systems was also shown to be cross-linked in some cases:

450   Deactivation of *acr* genes leads to an up-regulation of other efflux pump systems [151].

451   Furthermore, when AcrAB pump activity is impaired, AcrEF has been found to be

452   upregulated in the presence of quinolones [152] and overexpressed AcrD replaces AcrB to

453   form a tripartite assembly with AcrA-TolC (however, this replacement is repressed by AcrB-

454   specific substrates) [153]. These examples show how well the efflux pump part of the

455   bacterial proteome is coordinated and adjustable to compensate for loss of any component.

456   Regulation can furthermore happen on the post-transcriptional level. Both transcription

457   and translation attenuation can be abrogated by direct interaction of antibiotics with the

458 ribosome during translation upstream of resistance gene(s). The ribosome is temporarily stalled

459 so that an RNA secondary structure can form which (1) exposes the ribosome-binding site for

460 translation or (2) allows for the formation of an antiterminator structure, which enables the

461 RNA-polymerase to continue with transcription beyond a terminator [154]. As a consequence,

462 the resistance gene(s) can be translated or transcribed, respectively.

463 Other examples of post-transcriptional regulation involve sRNAs like SdsR. The latter

464 binds and thereby represses *tolC* mRNA in *E. coli* and *Salmonella* [155]. Other examples

465 include MdtEF regulation by DsrA in *E. coli* [156] and MtrF (part of MtrCDE) regulation by

466 NrrF in *Neisseria gonorrhoeae* [157]. Furthermore, sRNAs can 're-wire' two component

467 cascades and therewith indirectly influence expression level [158].

468 It has widely been assumed that an overexpression of pumps would impact on the cell.

469 For instance, overexpression of AcrAB in *Salmonella typhimurium* was suggested to come at

470 the expense of fitness and virulence [159]. Overexpression of AcrB also resulted in a switch in

471 *E. coli*'s carbon metabolism from a respiratory to fermentative mode [160]. In contrast to these

472 findings, overexpression of AcrAB in a RamR-deletion mutant of *Klebsiella pneumoniae*

473 revealed increased virulence [161] and overexpression of MtrCDE in *Neisseria gonorrhoeae*

474 increased fitness [162]. Furthermore, studies in *Pseudomonas aeruginosa* have shown that the

475 overexpression of the MexEF-OprN tripartite efflux pump system does not necessarily

476 decrease fitness – perhaps due to increased expression of genes encoding the nitrate respiratory

477 chain that might boost metabolic energy [163]. The increased presence of pumps in the

478 membrane may disturb pH homeostasis, which might be compensated by upregulated aerobic

479 respiration. This might account for the finding that, in an anaerobic environment, an increased

480 intracellular pH was measured in the over-expressing cells.

481 In addition to pump overexpression, mutants can account for increased pump activity:

482 A G288D substitution in AcrB's binding pocket changed the substrate specificity of the pump,

483 conferring ciprofloxacin resistance [164]. Mutations in binding pockets have also been

484 identified in clinical isolates [165].

485   Regulation can furthermore happen on the post-translational level. The activity of the

486 AcrAB-TolC pump for instance can be modulated by allosteric ligands. This is evident in the

487 increased resistance for some but not all of AcrB's substrates through the binding of a 49

488 amino-acid long alpha-helical protein described as AcrZ [166]. AcrZ expression is co-regulated

489 with AcrB by MarA, Rob, and SoxS [166]. The small protein binds to a groove in the inner

490 membrane-facing site of AcrB [166]. The exact mechanism by which AcrZ increases resistance

491 to tetracycline, puromycin and chloramphenicol remains to be explored.

492   Little is known about factors and conditions affecting pump assembly and disassembly.

493 The fact that outer membrane channels like TolC are used by multiple systems suggests

494 however that pump complexes assemble and disassemble in a transient fashion. Corresponding

495 findings from literature so far hint towards a regulatory role of the proton-motive-force for

496 pump disassembly (but not assembly). In particular, for the Neisseria MtrCDE system it was

497 found that whereas opening of the outer-membrane channel (MtrE) via interaction with the

498 membrane-fusion protein (MtrC) is energy-independent, drug export and complex dissociation

499 are dependent on active proton transport [167]. Studies of influx/efflux patterns by single

500 transporters in de-energised cells have demonstrated drug uptake driven by the drug gradient

501 in exchange for the export of protons (e.g. utilised in [168]). In order to counteract drug uptake

502 by the same system, pump complex disassembly and associated closure of the outer membrane

503 channel are needed. This could be related to the recently revealed 'twist-to-open' mechanism

504 mediated by the tip-to-tip interaction of TolC and AcrA [31] as well as with the observations

505 of rapid MexAB-OprM disassembly upon reaching thermodynamic equilibrium [169].

506 Interestingly however, experiments with a MexB mutant with a disrupted proton relay network

507   indicate that the assembly is still stable despite its inability to transport substrate [169, 170]. In

508   ABC transporters, it remains completely unclear how pump (dis-)assembly is governed.

509   Two possible regulatory mechanism of pump assembly and disassembly have been

510   suggested for the AcrAB/TolC system[171]. In one scenario, a drop in the periplasmic drug

511   concentration triggers the AcrB-trimer to acquire its pure LLL state, which lowers AcrA's

512   affinity for the AcrB trimer and henceforth shifts the equilibrium towards pump disassembly.

513   In a second scenario, tripartite (dis-)assembly could be pH-dependent given that the AcrAB

514   complex formation itself is favoured at a periplasmic pH of 6.0 but not at pH 7.5 [172].

515   Elevated periplasmic pH levels are indicative of a decreased proton-motive-force. A complex

516   disassembly at elevated pH/lowered pmf levels might therefore prevent the possibility of drug

517   uptake via the tripartite assembly itself. This might explain why the transport activity of the

518   AcrAB/TolC synchronises with fluctuation of pmf levels in the cell (high activity at high pmf

519   levels) [173-175].

520

521   **Summary and perspective**

522   The cell envelope of Gram-negative bacteria is a formidable barrier to the movement

523   of materials, and dedicated machinery is required to translocate substances including nutrients,

524   virulence factors and antibiotics through the cell envelope. The efflux of drugs and other

525   bactericidal compounds is achieved through tripartite nano-machines that transduce energy

526   derived from electrochemical transmembrane gradients or ATP hydrolysis to drive the efflux

527   process. The architecture of representative assemblies reveals common features for the RND

528   and ABC powered systems, and the mechanism of action involves a high degree of cooperation

529   between the protomers of the assembly.

530   Current understanding of the transport process by tripartite assemblies envisages that

531   the inner membrane component, sourcing energy for transport from either ATP hydrolysis

532   (ABC transporter) or electro-chemical gradients across the inner membrane, recognises and

533   binds substrates and guides these into the tripartite assembly for extrusion outside of the cell.

534   Depending on the system, the transporters reveal different degrees of poly-specificity, with

535   some recognising hundreds of chemically unrelated molecules (small compounds to medium-

536   sized peptides) whilst others are specialised in the transport of selected ions. Poly-specificity

537   is the result of multiple binding sites and of a variety of residues acting as potential binding

538   partners. The transport through the outer membrane is typically conducted via a channel protein

539   (e.g. TolC). The latter is 'opened' up for substrate-transport via the interaction with the

540   membrane fusion protein, which establishes the connection between the two separated

541   membrane components and transduces energy from the inner membrane component for

542   conformational changes in the entire tripartite system, including the opening of the outer

543   membrane channel.

544   One area of considerable interest with view to pump activity is the exploration of

545   specific locations of efflux pump assemblies within the membrane system. For the *E. coli*

546   AcrAB-TolC system, it has been shown that the older and more drug resistant mother cells

547   accumulate the pump assembly in clusters at the cell poles [176]. In relation with this

548   observation, lipid rafts might play a putative role in pump-activity and/or -specificity

549   regulation. Lipids can stabilise membrane protein oligomer formation [177] and also

550   facilitate large conformational changes within membrane proteins [178]. The role of lipids

551   for pump localization and regulation is an important topic for future investigations [179].

552   High-resolution structures have often been the starting point for functional exploration

553   towards a better and more detailed understanding of efflux mechanisms. Such understanding

554   can be the basis for inhibitor design (e.g. the pyranopyridine derivatives MBX2319, MBX2931,

555   MBX3132, and MBX3135 as AcrB inhibitors) [56, 180]. Pump inhibitors could be used as

556   novel antibiotic agents in the fight against multiple antibiotic resistance as well as for studies

557 towards a better structural and functional characterization of pumps in general. With the recent

558 emergence of high resolution structures of tripartite pumps, interesting functional findings can

559 be expected in the near future.

560 There are numerous important puzzle regarding efflux mechanisms. How much energy

561 is required for efflux, and how efficient is the process? Could some of the energy used to

562 discriminate transport substrates in a process that is analogous to kinetic proofreading?

563 Addressing these questions demands in vitro techniques with reconstituted purified protein in

564 liposomes, as established mostly for Gram-positive transporters in the past. These have been

565 challenging with tripartite system due to their assembly in double-membrane system [61]. A

566 successful functional reconstitution of a tripartite system has been achieved for the MexAB-

567 OprM system in liposomes so far and was utilised for in vitro activity studies [169].

568 Furthermore, the recently described reconstitution technique using lipid nanodiscs [181-183]

569 have opened new possibilities for both structural and functional analyses of membrane

570 proteins. Tripartite systems reveal a complex pattern of pre- and post-translational regulation

571 in response to the environment and physiological needs of the cell. An understanding of the

572 tripartite proteome-regulatory network as well as of the expression-induced effects on bacterial

573 physiology are needed in order to design effective drugs against tripartite assemblies. There is

574 still much to learn about how these systems are regulated, their functions, and their highly

575 cooperative mechanisms.

576

577

578 **Acknowledgements**

583   **References**

584   [1] Li X-Z, Elkins CA, Zgurskaya HI. Efflux-Mediated Antimicrobial Resistance in Bacteria:

585   Mechanisms, Regulation and Clinical Implications. Springer, 2016.

586   [2] Piddock LJ, White DG, Gensberg K, Pumbwe L, Griggs DJ. Evidence for an efflux pump

587   mediating multiple antibiotic resistance in Salmonella enterica serovar Typhimurium.

588   Antimicrob. Agents Chemother. 2000;44:3118-21.

589   [3] Piddock LJ, Johnson MM, Simjee S, Pumbwe L. Expression of efflux pump gene pmrA in

590   fluoroquinolone-resistant and-susceptible clinical isolates of Streptococcus pneumoniae.

591   Antimicrob. Agents Chemother. 2002;46:808-12.

592   [4] Piddock LJ. Clinically relevant chromosomally encoded multidrug resistance efflux pumps

593   in bacteria. Clin. Microbiol. Rev. 2006;19:382-402.

594   [5] Nishino K, Yamaguchi A. Analysis of a complete library of putative drug transporter genes

595   in Escherichia coli. J. Bacteriol. 2001;183:5803-12.

596   [6] Nishino K, Nikaido E, Yamaguchi A. Regulation and physiological function of multidrug

597   efflux pumps in Escherichia coli and Salmonella. Biochimica et Biophysica Acta (BBA)-

598   Proteins and Proteomics 2009;1794:834-43.

599   [7] Poole K. Efflux-mediated multiresistance in Gram-negative bacteria. Clin. Microbiol.

600   Infect. 2004;10:12-26.

601   [8] Tsukagoshi N, Aono R. Entry into and Release of Solvents byEscherichia coli in an

602   Organic-Aqueous Two-Liquid-Phase System and Substrate Specificity of the AcrAB-TolC

603   Solvent-Extruding Pump. J. Bacteriol. 2000;182:4803-10.

604   [9] White DG, Goldman JD, Demple B, Levy SB. Role of the acrAB locus in organic solvent

605   tolerance mediated by expression of marA, soxS, or robA in Escherichia coli. J. Bacteriol.

606   1997;179:6122-6.

607   [10] Franke S, Grass G, Rensing C, Nies DH. Molecular analysis of the copper-transporting

608   efflux system CusCFBA of Escherichia coli. J. Bacteriol. 2003;185:3804-12.

609   [11] Franke S, Grass G, Nies DH. The product of the ybdE gene of the Escherichia coli

610   chromosome is involved in detoxification of silver ions. Microbiology 2001;147:965-72.

611   [12] Borges-Walmsley MI, Beauchamp J, Kelly SM, Jumel K, Candlish D, Harding SE, et al.

612   Identification of oligomerization and drug-binding domains of the membrane fusion protein

613   EmrA. J. Biol. Chem. 2003;278:12903-12.

614   [13] Tanabe M, Szakonyi G, Brown KA, Henderson PJ, Nield J, Byrne B. The multidrug

615   resistance efflux complex, EmrAB from Escherichia coli forms a dimer in vitro. Biochem.

616   Biophys. Res. Commun. 2009;380:338-42.

617   [14] Poole K, Srikumar R. Multidrug efflux in Pseudomonas aeruginosa components,

618   mechanisms and clinical significance. Curr. Top. Med. Chem. 2001;1:59-71.

619   [15] Evans K, Passador L, Srikumar R, Tsang E, Nezezon J, Poole K. Influence of the MexAB-

620   OprM multidrug efflux system on quorum sensing in Pseudomonas aeruginosa. J. Bacteriol.

621   1998;180:5443-7.

622   [16] Keller L, Surette MG. Communication in bacteria: an ecological and evolutionary

623   perspective. Nature reviews. Microbiology 2006;4:249.

624   [17] Yang S, Lopez CR, Zechiedrich EL. Quorum sensing and multidrug transporters in

625   Escherichiacoli. Proc. Natl. Acad. Sci. U. S. A. 2006;103:2386-91.

626   [18] Severi E, Randle G, Kivlin P, Whitfield K, Young R, Moxon R, et al. Sialic acid transport

627   in Haemophilus influenzae is essential for lipopolysaccharide sialylation and serum resistance

628   and is dependent on a novel tripartite ATP-independent periplasmic transporter. Mol.

629   Microbiol. 2005;58:1173-85.

630   [19] Hirakata Y, Srikumar R, Poole K, Gotoh N, Suematsu T, Kohno S, et al. Multidrug efflux

631   systems play an important role in the invasiveness of Pseudomonas aeruginosa. J. Exp. Med.

632   2002;196:109-18.

633   [20] Koronakis V, Hughes C. Synthesis, maturation and export of the E. coli hemolysin. Med.

634   Microbiol. Immunol. 1996;185:65-71.

635   [21] Binet R, Létoffé S, Ghigo JM, Delepelaire P, Wandersman C. Protein secretion by Gram-

636   negative bacterial ABC exporters–a review. Gene 1997;192:7-11.

637   [22] Gilson L, Mahanty HK, Kolter R. Genetic analysis of an MDR-like export system: the

638   secretion of colicin V. The EMBO journal 1990;9:3875.

639   [23] Bina JE, Mekalanos JJ. Vibrio cholerae tolC is required for bile resistance and

640   colonization. Infect. Immun. 2001;69:4681-5.

641   [24] Boardman BK, Satchell KJF. Vibrio cholerae strains with mutations in an atypical type I

642   secretion system accumulate RTX toxin intracellularly. J. Bacteriol. 2004;186:8137-43.

643   [25] Join-Lambert O, Michea-Hamzehpour M, Köhler T, Chau F, Faurisson F, Dautrey S, et

644   al. Differential Selection of Multidrug Efflux Mutants by Trovafloxacin and Ciprofloxacin in

645   an Experimental Model ofPseudomonas aeruginosa Acute Pneumonia in Rats. Antimicrob.

646   Agents Chemother. 2001;45:571-6.

647   [26] Lee VT, Schneewind O. Protein secretion and the pathogenesis of bacterial infections.

648   Genes Dev. 2001;15:1725-52.

649   [27] Groisman EA, Mouslim C. Molecular mechanisms of Salmonella pathogenesis. Curr.

650   Opin. Infect. Dis. 2000;13:519-22.

651   [28] Van Dyk TK, Templeton LJ, Cantera KA, Sharpe PL, Sariaslani FS. Characterization of

652   the Escherichia coli AaeAB efflux pump: a metabolic relief valve? J. Bacteriol.

653   2004;186:7196-204.

654   [29] Murakami S, Nakashima R, Yamashita E, Yamaguchi A. Crystal structure of bacterial

655   multidrug efflux transporter AcrB. Nature 2002;419:587-93.

656   [30] Du D, Wang Z, James NR, Voss JE, Klimont E, Ohene-Agyei T, et al. Structure of the

657   AcrAB-TolC multidrug efflux pump. Nature 2014;509:512-5.

658   [31] Wang Z, Fan G, Hryc CF, Blaza JN, Serysheva II, Schmid MF, et al. An allosteric

659   transport mechanism for the AcrAB-TolC multidrug efflux pump. eLife 2017;6:e24905.

660   [32] Jeong H, Kim J-S, Song S, Shigematsu H, Yokoyama T, Hyun J, et al. Pseudoatomic

661   structure of the tripartite multidrug efflux pump AcrAB-TolC reveals the intermeshing

662   cogwheel-like interaction between AcrA and TolC. Structure 2016;24:272-6.

663   [33] Fitzpatrick AW, Llabrés S, Neuberger A, Blaza JN, Bai X-C, Okada U, et al. Structure of

664   the MacAB-TolC ABC-type tripartite multidrug efflux pump. Nature microbiology

665   2017;2:17070.

666   [34] Hayashi K, Nakashima R, Sakurai K, Kitagawa K, Yamasaki S, Nishino K, et al. AcrB-

667   AcrA fusion proteins that act as multidrug efflux transporters. J. Bacteriol. 2016;198:332-42.

668   [35] Tamura N, Murakami S, Oyama Y, Ishiguro M, Yamaguchi A. Direct interaction of

669   multidrug efflux transporter AcrB and outer membrane channel TolC detected via site-directed

670   disulfide cross-linking. Biochemistry 2005;44:11115-21.

671 [36] Lin HT, Bavro VN, Barrera NP, Frankish HM, Velamakanni S, van Veen HW, et al. MacB

672 ABC transporter is a dimer whose ATPase activity and macrolide-binding capacity are

673 regulated by the membrane fusion protein MacA. J. Biol. Chem. 2009;284:1145-54.

674 [37] Okada U, Yamashita E, Neuberger A, Morimoto M, van Veen HW, Murakami S. Crystal

675 structure of tripartite-type ABC transporter MacB from Acinetobacter baumannii. Nature

676 Communications 2017;8:1336.

677 [38] Crow A, Greene NP, Kaplan E, Koronakis V. Structure and mechanotransmission

678 mechanism of the MacB ABC transporter superfamily. Proceedings of the National Academy

679 of Sciences 2017;114:12572-7.

680 [39] Yang H-B, Hou W-T, Cheng M-T, Jiang Y-L, Chen Y, Zhou C-Z. Structure of a MacAB-

681 like efflux pump from Streptococcus pneumoniae. Nature communications 2018;9:196.

682 [40] Zhao X, Zhang K, Boquoi T, Hu B, Motaleb M, Miller KA, et al. Cryoelectron tomography

683 reveals the sequential assembly of bacterial flagella in Borrelia burgdorferi. Proceedings of the

684 National Academy of Sciences 2013;110:14390-5.

685 [41] Murakami S, Nakashima R, Yamashita E, Matsumoto T, Yamaguchi A. Crystal structures

686 of a multidrug transporter reveal a functionally rotating mechanism. Nature 2006;443:173-9.

687 [42] Seeger MA, Schiefner A, Eicher T, Verrey F, Diederichs K, Pos KM. Structural

688 asymmetry of AcrB trimer suggests a peristaltic pump mechanism. Science 2006;313:1295-8.

689   [43] Sennhauser G, Amstutz P, Briand C, Storchenegger O, Grütter MG. Drug export pathway

690   of multidrug exporter AcrB revealed by DARPin inhibitors. PLoS Biol. 2006;5:e7.

691   [44] Ntreh AT, Weeks JW, Nickels LM, Zgurskaya HI. Opening the Channel: the two

692   functional interfaces of Pseudomonas aeruginosa OpmH with the Triclosan Efflux pump

693   TriABC. J. Bacteriol. 2016;198:3176-85.

694   [45] Weeks JW, Bavro VN, Misra R. Genetic assessment of the role of AcrB β-hairpins in the

695   assembly of the TolC–AcrAB multidrug efflux pump of Escherichia coli. Mol. Microbiol.

696   2014;91:965-75.

697   [46] Andersen C, Koronakis E, Bokma E, Eswaran J, Humphreys D, Hughes C, et al. Transition

698   to the open state of the TolC periplasmic tunnel entrance. Proceedings of the National Academy

699   of Sciences 2002;99:11103-8.

700   [47] Augustus AM, Celaya T, Husain F, Humbard M, Misra R. Antibiotic-sensitive TolC

701   mutants and their suppressors. J. Bacteriol. 2004;186:1851-60.

702   [48] Bavro VN, Pietras Z, Furnham N, Pérez-Cano L, Fernández-Recio J, Pei XY, et al.

703   Assembly and channel opening in a bacterial drug efflux machine. Mol. Cell 2008;30:114-21.

704   [49] Koronakis V, Sharff A, Koronakis E, Luisi B, Hughes C. Crystal structure of the bacterial

705   membrane protein TolC central to multidrug efflux and protein export. Nature 2000;405:914.

706   [50] Balakrishnan L, Hughes C, Koronakis V. Substrate-triggered recruitment of the TolC

707   channel-tunnel during type I export of hemolysin by Escherichia coli. J. Mol. Biol.

708   2001;313:501-10.

709   [51] Eicher T, Cha H-j, Seeger MA, Brandstätter L, El-Delik J, Bohnert JA, et al. Transport of

710   drugs by the multidrug transporter AcrB involves an access and a deep binding pocket that are

711   separated by a switch-loop. Proceedings of the National Academy of Sciences 2012;109:5687-

712   92.

713   [52] Murakami S. Multidrug efflux transporter, AcrB—the pumping mechanism. Curr. Opin.

714   Struct. Biol. 2008;18:459-65.

715   [53] Oswald C, Tam H-K, Pos KM. Transport of lipophilic carboxylates is mediated by

716   transmembrane helix 2 in multidrug transporter AcrB. Nature communications 2016;7:13819.

717   [54] Eicher T, Seeger MA, Anselmi C, Zhou W, Brandstätter L, Verrey F, et al. Coupling of

718   remote alternating-access transport mechanisms for protons and substrates in the multidrug

719   efflux pump AcrB. Elife 2014;3:e03145.

720   [55] Du D, van Veen HW, Luisi BF. Assembly and operation of bacterial tripartite multidrug

721   efflux pumps. Trends Microbiol. 2015;23:311-9.

722   [56] Sjuts H, Vargiu AV, Kwasny SM, Nguyen ST, Kim H-S, Ding X, et al. Molecular basis

723   for inhibition of AcrB multidrug efflux pump by novel and powerful pyranopyridine

724   derivatives. Proceedings of the National Academy of Sciences 2016;113:3509-14.

725 [57] Vargiu AV, Ramaswamy VK, Malvacio I, Malloci G, Kleinekathöfer U, Ruggerone P.

726 Water-mediated interactions enable smooth substrate transport in a bacterial efflux pump.

727 Biochimica et Biophysica Acta (BBA)-General Subjects 2018.

728 [58] Nakashima R, Sakurai K, Yamasaki S, Nishino K, Yamaguchi A. Structures of the

729 multidrug exporter AcrB reveal a proximal multisite drug-binding pocket. Nature

730 2011;480:565-9.

731 [59] Zwama M, Yamasaki S, Nakashima R, Sakurai K, Nishino K, Yamaguchi A. Multiple

732 entry pathways within the efflux transporter AcrB contribute to multidrug recognition. Nature

733 communications 2018;9:124.

734 [60] Su C-C, Yin L, Kumar N, Dai L, Radhakrishnan A, Bolla JR, et al. Structures and transport

735 dynamics of a Campylobacter jejuni multidrug efflux pump. Nature Communications 2017;8.

736 [61] Tikhonova EB, Devroy VK, Lau SY, Zgurskaya HI. Reconstitution of the Escherichia coli

737 macrolide transporter: the periplasmic membrane fusion protein MacA stimulates the ATPase

738 activity of MacB. Mol. Microbiol. 2007;63:895-910.

739 [62] Lee A, Mao W, Warren MS, Mistry A, Hoshino K, Okumura R, et al. Interplay between

740 efflux pumps may provide either additive or multiplicative effects on drug resistance. J.

741 Bacteriol. 2000;182:3142-50.

742 [63] Li X-Z, Poole K, Nikaido H. Contributions of MexAB-OprM and an EmrE homolog to

743 intrinsic resistance of Pseudomonas aeruginosa to aminoglycosides and dyes. Antimicrob.

744 Agents Chemother. 2003;47:27-33.

745   [64] Tal N, Schuldiner S. A coordinated network of transporters with overlapping specificities

746   provides a robust survival strategy. Proceedings of the National Academy of Sciences

747   2009;106:9051-6.

748   [65] Elkins CA, Mullis LB. Mammalian steroid hormones are substrates for the major RND-

749   and MFS-type tripartite multidrug efflux pumps of Escherichia coli. J. Bacteriol.

750   2006;188:1191-5.

751   [66] Kobayashi N, Nishino K, Yamaguchi A. Novel Macrolide-Specific ABC-Type Efflux

752   Transporter inEscherichia coli. J. Bacteriol. 2001;183:5639-44.

753   [67] Vallet-Gely I, Novikov A, Augusto L, Liehl P, Bolbach G, Péchy-Tarr M, et al.

754   Association of hemolytic activity of Pseudomonas entomophila, a versatile soil bacterium, with

755   cyclic lipopeptide production. Appl. Environ. Microbiol. 2010;76:910-21.

756   [68] Cho H, Kang H. The PseEF efflux system is a virulence factor of Pseudomonas syringae

757   pv. syringae. The Journal of Microbiology 2012;50:79-90.

758   [69] Yamanaka H, Kobayashi H, Takahashi E, Okamoto K. MacAB is involved in the secretion

759   of Escherichia coli heat-stable enterotoxin II. J. Bacteriol. 2008;190:7693-8.

760   [70] Edward WY, McDermott G, Zgurskaya HI, Nikaido H, Koshland DE. Structural basis of

761   multiple drug-binding capacity of the AcrB multidrug efflux pump. Science 2003;300:976-80.

762   [71] Aller SG, Yu J, Ward A, Weng Y, Chittaboina S, Zhuo R, et al. Structure of P-glycoprotein

763   reveals a molecular basis for poly-specific drug binding. Science 2009;323:1718-22.

764 [72] Grkovic S, Brown MH, Roberts NJ, Paulsen IT, Skurray RA. QacR is a repressor protein

765 that regulates expression of theStaphylococcus aureus multidrug efflux pump QacA. J. Biol.

766 Chem. 1998;273:18665-73.

767 [73] Grkovic S, Brown MH, Schumacher MA, Brennan RG, Skurray RA. The staphylococcal

768 QacR multidrug regulator binds a correctly spaced operator as a pair of dimers. J. Bacteriol.

769 2001;183:7102-9.

770 [74] Schumacher MA, Miller MC, Grkovic S, Brown MH, Skurray RA, Brennan RG.

771 Structural mechanisms of QacR induction and multidrug recognition. Science 2001;294:2158-

772 63.

773 [75] Chufan EE, Kapoor K, Sim H-M, Singh S, Talele TT, Durell SR, et al. Multiple transport-

774 active binding sites are available for a single substrate on human P-glycoprotein (ABCB1).

775 PLoS One 2013;8:e82463.

776 [76] Lee M, Jun S-Y, Yoon B-Y, Song S, Lee K, Ha N-C. Membrane fusion proteins of type I

777 secretion system and tripartite efflux pumps share a binding motif for TolC in gram-negative

778 bacteria. PLoS One 2012;7:e40460.

779 [77] Morgan JL, Acheson JF, Zimmer J. Structure of a Type-1 Secretion System ABC

780 Transporter. Structure 2017;25:522-9.

781 [78] Mehmood S, Domene C, Forest E, Jault J-M. Dynamics of a bacterial multidrug ABC

782 transporter in the inward-and outward-facing conformations. Proceedings of the National

783 Academy of Sciences 2012;109:10832-6.

784   [79] Dawson RJ, Hollenstein K, Locher KP. Uptake or extrusion: crystal structures of full ABC

785   transporters suggest a common mechanism. Mol. Microbiol. 2007;65:250-7.

786   [80] Jardetzky O. Simple allosteric model for membrane pumps. Nature 1966;211:969-70.

787   [81] Locher KP, Lee AT, Rees DC. The E. coli BtuCD structure: a framework for ABC

788   transporter architecture and mechanism. Science 2002;296:1091-8.

789   [82] Mi W, Li Y, Yoon SH, Ernst RK, Walz T, Liao M. Structural basis of MsbA-mediated

790   lipopolysaccharide transport. Nature 2017.

791   [83] Oldham ML, Davidson AL, Chen J. Structural insights into ABC transporter mechanism.

792   Curr. Opin. Struct. Biol. 2008;18:726-33.

793   [84] Hollenstein K, Dawson RJ, Locher KP. Structure and mechanism of ABC transporter

794   proteins. Curr. Opin. Struct. Biol. 2007;17:412-8.

795   [85] Verhalen B, Dastvan R, Thangapandian S, Peskova Y, Koteiche HA, Nakamoto RK, et

796   al. Energy transduction and alternating access of the mammalian ABC transporter P-

797   glycoprotein. Nature 2017;543:738-41.

798   [86] Korkhov VM, Mireku SA, Locher KP. Structure of AMP-PNP-bound vitamin B^ sub 12^

799   transporter BtuCD-F. Nature 2012;490:367.

800   [87] Dawson RJ, Locher KP. Structure of a bacterial multidrug ABC transporter. Nature

801   2006;443:180.

802   [88] Ward A, Reyes CL, Yu J, Roth CB, Chang G. Flexibility in the ABC transporter MsbA:

803   Alternating access with a twist. Proceedings of the National Academy of Sciences

804   2007;104:19005-10.

805   [89] Jin MS, Oldham ML, Zhang Q, Chen J. Crystal structure of the multidrug transporter P-

806   glycoprotein from C. elegans. Nature 2012;490:566.

807   [90] Mishra S, Verhalen B, Stein RA, Wen P-C, Tajkhorshid E, Mchaourab HS.

808   Conformational dynamics of the nucleotide binding domains and the power stroke of a

809   heterodimeric ABC transporter. Elife 2014;3:e02740.

810   [91] McCormick JW, Vogel PD, Wise JG. Multiple drug transport pathways through human

811   P-glycoprotein. Biochemistry 2015;54:4374-90.

812   [92] Jones PM, George AM. Opening of the ADP-bound active site in the ABC transporter

813   ATPase dimer: Evidence for a constant contact, alternating sites model for the catalytic cycle.

814   Proteins: Structure, Function, and Bioinformatics 2009;75:387-96.

815   [93] Zutz A, Hoffmann J, Hellmich UA, Glaubitz C, Ludwig B, Brutschy B, et al. Asymmetric

816   ATP hydrolysis cycle of the heterodimeric multidrug ABC transport complex TmrAB from

817   Thermus thermophilus. J. Biol. Chem. 2011;286:7104-15.

818   [94] Lubelski J, van Merkerk R, Konings WN, Driessen AJ. Nucleotide-binding sites of the

819   heterodimeric LmrCD ABC-multidrug transporter of Lactococcus lactis are asymmetric.

820   Biochemistry 2006;45:648-56.

821   [95] Hohl M, Briand C, Grütter MG, Seeger MA. Crystal structure of a heterodimeric ABC

822   transporter in its inward-facing conformation. Nat. Struct. Mol. Biol. 2012;19:395-402.

823   [96] George AM, Jones PM. Perspectives on the structure–function of ABC transporters: the

824   switch and constant contact models. Prog. Biophys. Mol. Biol. 2012;109:95-107.

825   [97] Tombline G, Senior AE. The occluded nucleotide conformation of P-glycoprotein. J.

826   Bioenerg. Biomembr. 2005;37:497-500.

827   [98] Siarheyeva A, Liu R, Sharom FJ. Characterization of an Asymmetric Occluded State of

828   P-glycoprotein with Two Bound Nucleotides IMPLICATIONS FOR CATALYSIS. J. Biol.

829   Chem. 2010;285:7575-86.

830   [99] Linhartová I, Bumba L, Mašín J, Basler M, Osička R, Kamanová J, et al. RTX proteins: a

831   highly diverse family secreted by a common mechanism. FEMS Microbiol. Rev.

832   2010;34:1076-112.

833   [100] Binet R, Wandersman C. Protein secretion by hybrid bacterial ABC-transporters: specific

834   functions of the membrane ATPase and the membrane fusion protein. The EMBO journal

835   1995;14:2298.

836   [101] Delepelaire P. Type I secretion in gram-negative bacteria. Biochimica et Biophysica Acta

837   (BBA)-Molecular Cell Research 2004;1694:149-61.

838   [102] Fuche F, Vianney A, Andrea C, Doublet P, Gilbert C. Functional type 1 secretion system

839   involved in Legionella pneumophila virulence. J. Bacteriol. 2015;197:563-71.

840   [103] Debarbieux L, Wandersman C. Folded HasA inhibits its own secretion through its ABC

841   exporter. The EMBO journal 2001;20:4657-63.

842   [104] Bakkes PJ, Jenewein S, Smits SH, Holland IB, Schmitt L. The rate of folding dictates

843   substrate secretion by the Escherichia coli hemolysin type 1 secretion system. J. Biol. Chem.

844   2010;285:40573-80.

845   [105] Kanonenberg K, Schwarz CK, Schmitt L. Type I secretion systems–a story of

846   appendices. Res. Microbiol. 2013;164:596-604.

847   [106] Thomas S, Holland IB, Schmitt L. The type 1 secretion pathway—the hemolysin system

848   and beyond. Biochimica et Biophysica Acta (BBA)-Molecular Cell Research 2014;1843:1629-

849   41.

850   [107] Koronakis V, Koronakis E, Hughes C. Isolation and analysis of the C-terminal signal

851   directing export of Escherichia coli hemolysin protein across both bacterial membranes. The

852   EMBO journal 1989;8:595.

853   [108] Chervaux C, Sauvonnet N, Le Clainche A, Kenny B, Hunt AL, Broome-Smith JK, et al.

854   Secretion of active β-lactamase to the medium mediated by the Escherichia coli haemolysin

855   transport pathway. Molecular and General Genetics MGG 1995;249:237-45.

856   [109] Gray L, Mackman N, Nicaud J-M, Holland I. The carboxy-terminal region of haemolysin

857   2001 is required for secretion of the toxin fromEscherichia coli. Molecular and General

858   Genetics MGG 1986;205:127-33.

859   [110] Letoffe S, Delepelaire P, Wandersman C. Protein secretion in gram-negative bacteria:

860   assembly of the three components of ABC protein-mediated exporters is ordered and promoted

861   by substrate binding. The EMBO journal 1996;15:5804.

862   [111] Oldham ML, Hite RK, Steffen AM, Damko E, Li Z, Walz T, et al. A mechanism of viral

863   immune evasion revealed by cryo-EM analysis of the TAP transporter. Nature 2016;529:537.

864   [112] Delepelaire P. PrtD, the integral membrane ATP-binding cassette component of the

865   Erwinia chrysanthemi metalloprotease secretion system, exhibits a secretion signal-regulated

866   ATPase activity. J. Biol. Chem. 1994;269:27952-7.

867   [113] Masi M, Wandersman C. Multiple signals direct the assembly and function of a type 1

868   secretion system. J. Bacteriol. 2010;192:3861-9.

869   [114] Thanabalu T, Koronakis E, Hughes C, Koronakis V. Substrate-induced assembly of a

870   contiguous channel for protein export from E. coli: reversible bridging of an inner-membrane

871   translocase to an outer membrane exit pore. The EMBO Journal 1998;17:6487-96.

872   [115] Kupersztoch Y, Tachias K, Moomaw C, Dreyfus L, Urban R, Slaughter C, et al. Secretion

873   of methanol-insoluble heat-stable enterotoxin (STB): energy-and secA-dependent conversion

874   of pre-STB to an intermediate indistinguishable from the extracellular toxin. J. Bacteriol.

875   1990;172:2427-32.

876   [116] Okamoto K, Takahara M. Synthesis of Escherichia coli heat-stable enterotoxin STp as a

877   pre-pro form and role of the pro sequence in secretion. J. Bacteriol. 1990;172:5260-5.

878   [117] Yamanaka H, Nomura T, Fujii Y, Okamoto K. Extracellular secretion of Escherichia coli

879   heat-stable enterotoxin I across the outer membrane. J. Bacteriol. 1997;179:3383-90.

880   [118] Lee J-Y, Kinch LN, Borek DM, Wang J, Wang J, Urbatsch IL, et al. Crystal structure of

881   the human sterol transporter ABCG5/ABCG8. Nature 2016;533:561-4.

882   [119] Locher KP. Mechanistic diversity in ATP-binding cassette (ABC) transporters. Nat.

883   Struct. Mol. Biol. 2016;23:487-93.

884   [120] Reimann S, Poschmann G, Kanonenberg K, Stühler K, Smits SH, Schmitt L. Interdomain

885   regulation of the ATPase activity of the ABC transporter haemolysin B from Escherichia coli.

886   Biochem. J. 2016;473:2471-83.

887   [121] Zhang F, Sheps J, Ling V. Complementation of transport-deficient mutants of

888   Escherichia coli alpha-hemolysin by second-site mutations in the transporter hemolysin B. J.

889   Biol. Chem. 1993;268:19889-95.

890   [122] Sheps JA, Cheung I, Ling V. Hemolysin transport in Escherichia coli. Point mutants in

891   HlyB compensate for a deletion in the predicted amphiphilic helix region of the HlyA signal.

892   J. Biol. Chem. 1995;270:14829-34.

893   [123] Delepelaire P, Wandersman C. Protein secretion in gram-negative bacteria. The

894   extracellular metalloprotease B from Erwinia chrysanthemi contains a C-terminal secretion

895   signal analogous to that of Escherichia coli alpha-hemolysin. J. Biol. Chem. 1990;265:17118-

896   25.

897   [124] Blair JM, Richmond GE, Piddock LJ. Multidrug efflux pumps in Gram-negative bacteria

898   and their role in antibiotic resistance. Future Microbiol. 2014;9:1165-77.

899   [125] Hernando-Amado S, Blanco P, Alcalde-Rico M, Corona F, Reales-Calderón JA, Sánchez

900   MB, et al. Multidrug efflux pumps as main players in intrinsic and acquired resistance to

901   antimicrobials. Drug Resistance Updates 2016;28:13-27.

902   [126] Stock AM, Robinson VL, Goudreau PN. Two-component signal transduction. Annu.

903   Rev. Biochem. 2000;69:183-215.

904   [127] Hoch JA. Two-component and phosphorelay signal transduction. Curr. Opin. Microbiol.

905   2000;3:165-70.

906   [128] Piepenbreier H, Fritz G, Gebhard S. Transporters as information processors in bacterial

907   signalling pathways. Mol. Microbiol. 2017;104:1-15.

908   [129] Sun J-R, Jeng W-Y, Perng C-L, Yang Y-S, Soo P-C, Chiang Y-S, et al. Single amino

909   acid substitution Gly186Val in AdeS restores tigecycline susceptibility of Acinetobacter

910   baumannii. J. Antimicrob. Chemother. 2016;71:1488-92.

911   [130] Marchand I, Damier-Piolle L, Courvalin P, Lambert T. Expression of the RND-type

912   efflux pump AdeABC in Acinetobacter baumannii is regulated by the AdeRS two-component

913   system. Antimicrob. Agents Chemother. 2004;48:3298-304.

914   [131] Nowak J, Schneiders T, Seifert H, Higgins PG. The Asp20-to-Asn substitution in the

915   response regulator AdeR leads to enhanced efflux activity of AdeB in Acinetobacter

916   baumannii. Antimicrob. Agents Chemother. 2016;60:1085-90.

917   [132] Koteva K, Hong H-J, Wang XD, Nazi I, Hughes D, Naldrett MJ, et al. A vancomycin

918   photoprobe identifies the histidine kinase VanSsc as a vancomycin receptor. Nat. Chem. Biol.

919   2010;6:327-9.

920   [133] Fritz G, Dintner S, Treichel NS, Radeck J, Gerland U, Mascher T, et al. A new way of

921   sensing: need-based activation of antibiotic resistance by a flux-sensing mechanism. MBio

922   2015;6:e00975-15.

923   [134] Poole K, Gilmour C, Farha MA, Mullen E, Lau CH-F, Brown ED. Potentiation of

924   aminoglycoside activity in Pseudomonas aeruginosa by targeting the AmgRS envelope stress-

925   responsive two-component system. Antimicrob. Agents Chemother. 2016;60:3509-18.

926   [135] Chang T-Y, Huang B-J, Sun J-R, Perng C-L, Chan M-C, Yu C-P, et al. AdeR protein

927   regulates adeABC expression by binding to a direct-repeat motif in the intercistronic spacer.

928   Microbiol. Res. 2016;183:60-7.

929   [136] Nishino K, Nikaido E, Yamaguchi A. Regulation of multidrug efflux systems involved

930   in multidrug and metal resistance of Salmonella enterica serovar Typhimurium. J. Bacteriol.

931   2007;189:9066-75.

932   [137] Hirakawa H, Inazumi Y, Masaki T, Hirata T, Yamaguchi A. Indole induces the

933   expression of multidrug exporter genes in Escherichia coli. Mol. Microbiol. 2005;55:1113-26.

934   [138] Ma D, Alberti M, Lynch C, Nikaido H, Hearst JE. The local repressor AcrR plays a

935   modulating role in the regulation of acrAB genes of Escherichia coli by global stress signals.

936   Mol. Microbiol. 1996;19:101-12.

937   [139] Alekshun MN, Levy SB. Regulation of chromosomally mediated multiple antibiotic

938   resistance: the mar regulon. Antimicrob. Agents Chemother. 1997;41:2067.

939   [140] Chollet R, Chevalier J, Bollet C, Pages J-M, Davin-Regli A. RamA is an alternate

940   activator of the multidrug resistance cascade in Enterobacter aerogenes. Antimicrob. Agents

941   Chemother. 2004;48:2518-23.

942   [141] Ruzin A, Visalli MA, Keeney D, Bradford PA. Influence of transcriptional activator

943   RamA on expression of multidrug efflux pump AcrAB and tigecycline susceptibility in

944   Klebsiella pneumoniae. Antimicrob. Agents Chemother. 2005;49:1017-22.

945   [142] Abouzeed YM, Baucheron S, Cloeckaert A. ramR mutations involved in efflux-mediated

946   multidrug resistance in Salmonella enterica serovar Typhimurium. Antimicrob. Agents

947   Chemother. 2008;52:2428-34.

948   [143] Yamasaki S, Nikaido E, Nakashima R, Sakurai K, Fujiwara D, Fujii I, et al. The crystal

949   structure of multidrug-resistance regulator RamR with multiple drugs. Nature communications

950   2013;4.

951   [144] Chen H, Hu J, Chen PR, Lan L, Li Z, Hicks LM, et al. The Pseudomonas aeruginosa

952   multidrug efflux regulator MexR uses an oxidation-sensing mechanism. Proceedings of the

953   National Academy of Sciences 2008;105:13586-91.

954   [145] Li M, Gu R, Su C-C, Routh MD, Harris KC, Jewell ES, et al. Crystal structure of the

955   transcriptional regulator AcrR from Escherichia coli. J. Mol. Biol. 2007;374:591-603.

956   [146] Wilke MS, Heller M, Creagh AL, Haynes CA, McIntosh LP, Poole K, et al. The crystal

957   structure of MexR from Pseudomonas aeruginosa in complex with its antirepressor ArmR.

958   Proceedings of the National Academy of Sciences 2008;105:14832-7.

959   [147] Yamada J, Yamasaki S, Hirakawa H, Hayashi-Nishino M, Yamaguchi A, Nishino K.

960   Impact of the RNA chaperone Hfq on multidrug resistance in Escherichia coli. J. Antimicrob.

961   Chemother. 2010;65:853-8.

962   [148] Grkovic S, Brown MH, Skurray RA. Regulation of bacterial drug export systems.

963   Microbiol. Mol. Biol. Rev. 2002;66:671-701.

964   [149] Jeannot K, Sobel ML, El Garch F, Poole K, Plésiat P. Induction of the MexXY efflux

965   pump in Pseudomonas aeruginosa is dependent on drug-ribosome interaction. J. Bacteriol.

966   2005;187:5341-6.

967   [150] Juarez P, Jeannot K, Plésiat P, Llanes C. Toxic Electrophiles Induce Expression of the

968   Multi-Drug Efflux Pump MexEF-OprN in Pseudomonas aeruginosa Through a Novel

969   Transcriptional Regulator, CmrA. Antimicrob. Agents Chemother. 2017;AAC. 00585-17.

970   [151] Blair JM, Smith HE, Ricci V, Lawler AJ, Thompson LJ, Piddock LJ. Expression of

971   homologous RND efflux pump genes is dependent upon AcrB expression: implications for

972   efflux and virulence inhibitor design. J. Antimicrob. Chemother. 2014;70:424-31.

973   [152] Zhang C-Z, Chang M-X, Yang L, Liu Y-Y, Chen P-X, Jiang H-X. Upregulation of AcrEF

974   in Quinolone Resistance Development in Escherichia coli When AcrAB-TolC Function Is

975   Impaired. Microbial Drug Resistance 2017.

976   [153] Yamamoto K, Tamai R, Yamazaki M, Inaba T, Sowa Y, Kawagishi I. Substrate-

977   dependent dynamics of the multidrug efflux transporter AcrB of Escherichia coli. Sci. Rep.

978   2016;6:21909.

979   [154] Dersch P, Khan MA, Mühlen S, Görke B. Roles of regulatory RNAs for antibiotic

980   resistance in bacteria and their potential value as novel drug targets. Front. Microbiol. 2017;8.

981   [155] Parker A, Gottesman S. Small RNA regulation of TolC, the outer membrane component

982   of bacterial multidrug transporters. J. Bacteriol. 2016;198:1101-13.

983   [156] Nishino K, Yamasaki S, Hayashi-Nishino M, Yamaguchi A. Effect of overexpression of

984   small non-coding DsrA RNA on multidrug efflux in Escherichia coli. J. Antimicrob.

985   Chemother. 2010;66:291-6.

986   [157] Jackson LA, Pan J-C, Day MW, Dyer DW. Control of RNA stability by NrrF, an iron-

987   regulated small RNA in Neisseria gonorrhoeae. J. Bacteriol. 2013;195:5166-73.

988   [158] Göpel Y, Görke B. Rewiring two-component signal transduction with small RNAs. Curr.

989   Opin. Microbiol. 2012;15:132-9.

990 [159] Bailey AM, Ivens A, Kingsley R, Cottell JL, Wain J, Piddock LJ. RamA, a member of

991 the AraC/XylS family, influences both virulence and efflux in Salmonella enterica serovar

992 Typhimurium. J. Bacteriol. 2010;192:1607-16.

993 [160] Zampieri M, Enke T, Chubukov V, Ricci V, Piddock L, Sauer U. Metabolic constraints

994 on the evolution of antibiotic resistance. Mol. Syst. Biol. 2017;13:917.

995 [161] De Majumdar S, Yu J, Fookes M, McAteer SP, Llobet E, Finn S, et al. Elucidation of the

996 RamA regulon in Klebsiella pneumoniae reveals a role in LPS regulation. PLoS Pathog.

997 2015;11:e1004627.

998 [162] Ohneck EA, Goytia M, Rouquette-Loughlin CE, Joseph SJ, Read TD, Jerse AE, et al.

999 Overproduction of the MtrCDE efflux pump in Neisseria gonorrhoeae produces unexpected

1000 changes in cellular transcription patterns. Antimicrob. Agents Chemother. 2015;59:724-6.

1001 [163] Pacheco JO, Alvarez-Ortega C, Rico MA, Martínez JL. Metabolic Compensation of

1002 Fitness Costs Is a General Outcome for Antibiotic-Resistant Pseudomonas aeruginosa Mutants

1003 Overexpressing Efflux Pumps. mBio 2017;8:e00500-17.

1004 [164] Blair JM, Bavro VN, Ricci V, Modi N, Cacciotto P, Kleinekathöfer U, et al. AcrB drug-

1005 binding pocket substitution confers clinically relevant resistance and altered substrate

1006 specificity. Proceedings of the National Academy of Sciences 2015;112:3511-6.

1007 [165] Yao H, Shen Z, Wang Y, Deng F, Liu D, Naren G, et al. Emergence of a potent multidrug

1008 efflux pump variant that enhances Campylobacter resistance to multiple antibiotics. mBio

1009 2016;7:e01543-16.

1010   [166] Hobbs EC, Yin X, Paul BJ, Astarita JL, Storz G. Conserved small protein associates with

1011   the multidrug efflux pump AcrB and differentially affects antibiotic resistance. Proceedings of

1012   the National Academy of Sciences 2012;109:16696-701.

1013   [167] Janganan TK, Bavro VN, Zhang L, Borges-Walmsley MI, Walmsley AR. Tripartite

1014   efflux pumps: energy is required for dissociation, but not assembly or opening of the outer

1015   membrane channel of the pump. Mol. Microbiol. 2013;88:590-602.

1016   [168] Neuberger A, van Veen HW. Hoechst 33342 is a hidden "Janus" amongst substrates for

1017   the multidrug efflux pump LmrP. PLoS One 2015;10:e0141991.

1018   [169] Verchère A, Dezi M, Adrien V, Broutin I, Picard M. In vitro transport activity of the

1019   fully assembled MexAB-OprM efflux pump from Pseudomonas aeruginosa. Nature

1020   communications 2015;6.

1021   [170] Enguéné VYN, Verchère A, Phan G, Broutin I, Picard M. Catch me if you can: a

1022   biotinylated proteoliposome affinity assay for the investigation of assembly of the MexA-

1023   MexB-OprM efflux pump from Pseudomonas aeruginosa. Front. Microbiol. 2015;6.

1024   [171] Müller RT, Pos KM. The assembly and disassembly of the AcrAB-TolC three-

1025   component multidrug efflux pump. Biol. Chem. 2015;396:1083-9.

1026   [172] Tikhonova EB, Yamada Y, Zgurskaya HI. Sequential mechanism of assembly of

1027   multidrug efflux pump AcrAB-TolC. Chem. Biol. 2011;18:454-63.

1028 [173] Cherepanov DA, Feniouk BA, Junge W, Mulkidjanian AY. Low dielectric permittivity

1029 of water at the membrane interface: effect on the energy coupling mechanism in biological

1030 membranes. Biophys. J. 2003;85:1307-16.

1031 [174] Cherepanov DA, Junge W, Mulkidjanian AY. Proton transfer dynamics at the

1032 membrane/water interface: dependence on the fixed and mobile pH buffers, on the size and

1033 form of membrane particles, and on the interfacial potential barrier. Biophys. J. 2004;86:665-

1034 80.

1035 [175] Kralj JM, Hochbaum DR, Douglass AD, Cohen AE. Electrical spiking in Escherichia

1036 coli probed with a fluorescent voltage-indicating protein. Science 2011;333:345-8.

1037 [176] Bergmiller T, Andersson AM, Tomasek K, Balleza E, Kiviet DJ, Hauschild R, et al.

1038 Biased partitioning of the multidrug efflux pump AcrAB-TolC underlies long-lived phenotypic

1039 heterogeneity. Science 2017;356:311-5.

1040 [177] Gupta K, Donlan JA, Hopper JT, Uzdavinys P, Landreh M, Struwe WB, et al. The role

1041 of interfacial lipids in stabilizing membrane protein oligomers. Nature 2017;1-4.

1042 [178] Landreh M, Marklund EG, Uzdavinys P, Degiacomi MT, Coincon M, Gault J, et al.

1043 Integrating mass spectrometry with MD simulations reveals the role of lipids in Na+/H+

1044 antiporters. Nature communications 2017;8.

1045 [179] Neumann J, Rose-Sperling D, Hellmich UA. Diverse relations between ABC transporters

1046 and lipids: An overview. Biochimica et Biophysica Acta (BBA)-Biomembranes

1047 2017;1859:605-18.

1048   [180] Vargiu AV, Ruggerone P, Opperman TJ, Nguyen ST, Nikaido H. Molecular mechanism

1049   of MBX2319 inhibition of Escherichia coli AcrB multidrug efflux pump and comparison with

1050   other inhibitors. Antimicrob. Agents Chemother. 2014;58:6224-34.

1051   [181] Denisov IG, Sligar SG. Nanodiscs for structural and functional studies of membrane

1052   proteins. Nat. Struct. Mol. Biol. 2016;23:481-6.

1053   [182] Frauenfeld J, Löving R, Armache J-P, Sonnen AF, Guettou F, Moberg P, et al. A saposin-

1054   lipoprotein nanoparticle system for membrane proteins. Nature methods 2016;13:345-51.

1055   [183] Daury L, Orange F, Taveau J-C, Verchère A, Monlezun L, Gounou C, et al. Tripartite

1056   assembly of RND multidrug efflux pumps. Nature communications 2016;7:10731.

1057